1

2

3

4

5

6

7 **Location specific small RNA annealing to the HCV 5' UTR promotes Hepatitis C Virus**

8 **replication by favoring IRES formation and stimulating virus translation**

9

10 **Rasika D. Kunden[1], Sarah Ghezelbash[1], Juveriya Q. Khan[1], and Joyce A. Wilson[1,*]**

11

12 [1]Department of Biochemistry, Microbiology and Immunology, University of Saskatchewan,

13 Saskatoon, Saskatchewan, S7N 5E5, Canada

14 Keywords: Hepatitis C Virus, miR-122, siRNA, 5' untranslated region, Argonaute 2, knockout.

15

16 * To whom correspondence should be addressed:

17

18 Tel: +1 306 966 1280

19 Fax: +1 306 966 4298

20 Email: joyce.wilson@usask.ca

21

22

23

24

25

26

27

28 **ABSTRACT:**

29

30 Hepatitis C virus (HCV) genome replication requires annealing of a liver specific small-

31 RNA, miR-122 to 2 sites on 5' untranslated region (UTR). Annealing has been reported to a)

32 stabilize the genome, b) promote translation, and c) induce the canonical HCV 5' UTR Internal

33 Ribosome Entry Site (IRES) structure. In this report we identify the relative impact of small RNA

34 annealing on the three functions ascribed to miR-122 and generate a mechanistic model for miR-

35 122 promotion of HCV. First, we identified that perfectly complementary small RNAs that anneal

36 to different locations on the HCV 5' UTR stimulate replication with varying efficiencies and

37 mapped the region on the HCV genome to which small RNA annealing promotes virus replication.

38 Second, by using a panel of small RNAs that promote with varying efficiencies we link HCV

39 replication induction with translation stimulation and 5' UTR RNA structure modifications.

40 However, replication promotion was not linked to genome stabilization since all small RNAs

41 tested could stabilize the viral genome regardless of their ability to promote replication. Thus, we

42 propose that miR-122 annealing promotes HCV replication primarily by activating the HCV IRES

43 and stimulating translation, and that miR-122-induced HCV genome stabilization is insufficient

44 alone but enhances virus replication.

45

46

47

Graphical Abstract
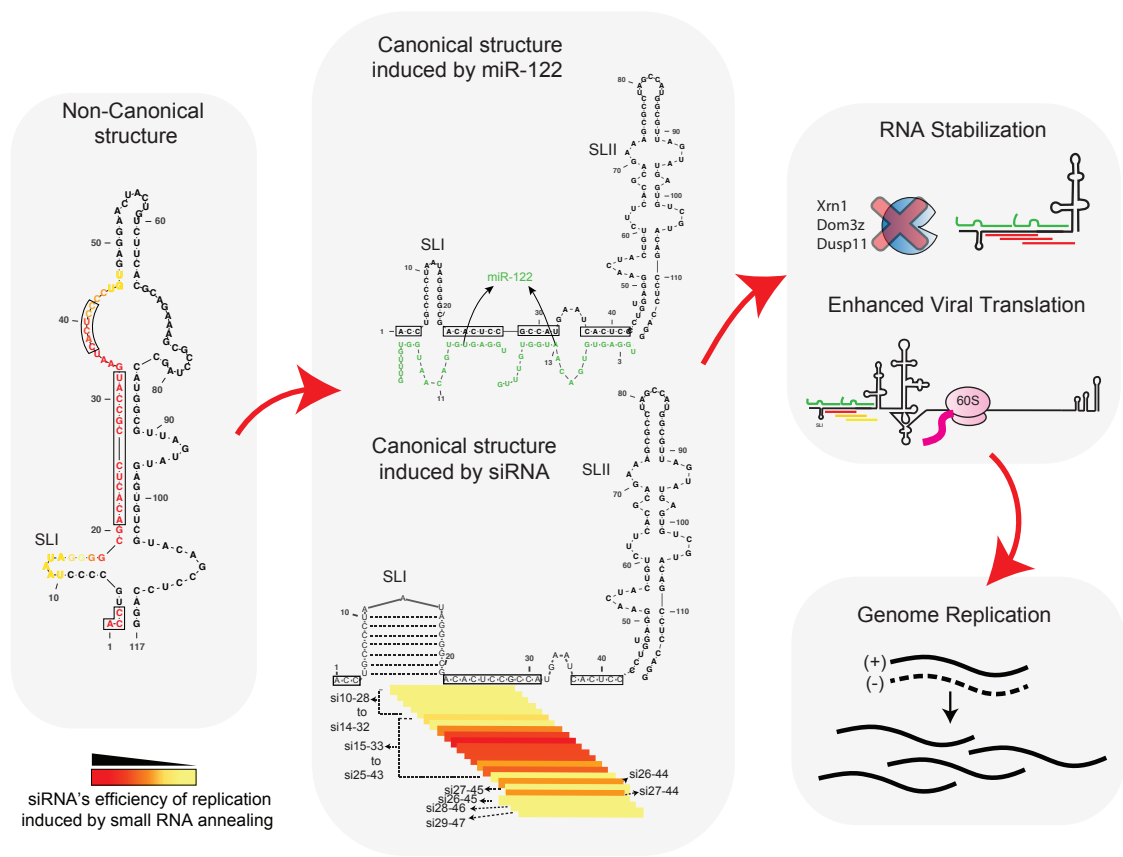
INTRODUCTION:

Hepatitis C Virus (HCV) is a flavivirus that causes chronic infections of the liver and can lead to liver cirrhosis and hepatocellular carcinoma (1, 2). The genome of HCV is a 9.6 kb long positive sense RNA that consists of a 5' untranslated region (UTR), a polyprotein coding region, and a 3'UTR region. The 5' and 3' UTRs are highly structured and required for genome translation and replication (3, 4).

The 5'UTR is a structured RNA that forms 4 stem loops (SL), SLI, SLII, SLIII and SLIV. SLII, SLIII and SLIV comprise the internal ribosomal entry site (IRES) that drives cap-independent HCV translation (Figure 1A) (5, 6). SLII is divided into two parts, SLIIa which induces SLII to form a bent structure that directs SLIIb, to the ribosomal E-site in the head region of the 40S subunit, facilitating 80S ribosome assembly (7–9). The first 42 nucleotides on the 5'UTR are not considered part of the IRES and forms SLI and an RNA structured element created by annealing of two copies of microRNA-122 (miR-122), a host microRNA found in human liver cells (10–13). This tri-molecular structure is required for virus replication (11–14).

MicroRNAs (miRNAs) are small RNAs about 21-23 nucleotides long and are central to mRNA regulated by miRNA gene silencing (15, 16). miRNAs silence genes in association with a host Argonaute (Ago) protein within an RNA induced silencing complex (RISC) and directs the protein complex to the 3' UTR of an mRNA by annealing with imperfect sequence complementarity (17). miRNAs target an mRNA by annealing to an approximately 6-7 nucleotide seed site binding at the 5' end of the miRNA and an accessory site binding on the 3'end (18). This leaves a loop of mismatched nucleotides between the seed and accessory sites and overhangs on the 5' and 3' ends of the miRNA that do not bind to the target mRNA. Such complex miRNA:target RNA interactions regulates the expression of multiple mRNAs by inducing translation suppression

71 and degradation of target mRNA (19). Two copies of miR-122 anneal in conjunction with Ago to

72 the HCV genome in a similar manner, including seed and accessory binding sites (20) but in this

73 case promotes instead of silencing the viral genome.

74   HCV replication is undetectable in the absence of miR-122 and the mechanism behind

75 miR-122's stimulatory effect is not fully understood. miR-122 stabilizes the viral RNA by

76 protecting it from degradation by host exonuclease Xrn1, and phosphatases Dom3Z and DUSP11

77 (21–23). However, simultaneous knock-down of these three enzymes cannot completely rescue

78 HCV replication in the absence of miR-122, suggesting that other roles exist (23). miR-122 also

79 promotes HCV translation and recent reports hypothesize that miR-122 modifies the HCV genome

80 to induce the canonical 5'UTR IRES structure (Figure 1B and C) (12, 13, 24). Finally, miR-122

81 has been reported to directly induce genome amplification (25, 26). However, the relative impact

82 of these functions on miR-122 directed HCV replication promotion is unknown (27).

83   We previously showed that annealing of small interfering RNAs (siRNA) to the HCV 5'

84 UTR can mimic the pro-viral activity of miR-122 (13). Like miRNAs, siRNAs are also 21–23

85 nucleotides in length and associate with Ago proteins, but based on associating with Ago2 and

86 perfect sequence match with their targets, induce mRNA cleavage and gene knockdown (28, 29).

87 However, when siRNA cleavage activity was blocked by using Ago2 knockout cells, siRNAs that

88 anneal to the miR-122 binding region on the HCV genome they promoted virus replication, some

89 as efficiently as miR-122. That siRNA annealing promoted HCV, suggested that the complex

90 annealing pattern formed by miR-122 on the HCV genome was not required for the pro-viral

91 activity. It also provided a method to assess the impact of small RNA annealing to other locations

92 on the genome on HCV replication (13). Using a panel of HCV genome-targeting siRNAs, we

93 found that annealing between nucleotides 1 and 44 in HCV 5'UTR, promoted HCV replication,

94 and annealing within the IRES, NS5B and 3'UTR regions did not. We also found that siRNAs that

95 annealed to different locations on the 5' UTR promoted virus replication with different efficiencies

96 and the efficiency correlated with their ability to stimulate translation and their predicted ability to

97 induce the canonical SLII structure of the HCV IRES. Finally, like miR-122, annealing of the

98 siRNAs to the 5' UTR also stabilized the viral genome, but the siRNAs did so regardless of

99 whether they could promote replication, suggesting that genome stabilization alone is insufficient

100 for HCV replication promotion. Thus, our current model for the pro-viral mechanism of miR-122

101 replication posits that its primary role is to stimulate translation by inducing a 5' UTR RNA

102 structural switch element to form the canonical HCV IRES structure, and that genome stabilization

103 is its secondary role that is insufficient alone, but enhances replication induced by translation

104 stimulation.

105

106

107 **MATERIALS AND METHODS:**

108 **Plasmids**

109 Full-length HCV Renilla Luciferase (Rluc) reporter genome constructs pJ6/JFH-1 RLuc (p7-

110 RLuc2A) and the non-replicative version pJ6/JFH-1 RLuc (p7-RLuc2A) GNN were provided by

111 Dr. C. M. Rice (30). For translation suppression assays the miR-122 suppression firefly luciferase

112 (Fluc) reporter plasmid, pFLuc JFH-1 5'UTR × 2 (11) was modified to contain a single copy of

113 the complete 5'UTR (pFluc JFH-1 5'UTR) or NS5B-3'UTR (pFluc JFH-1 NS5B-3'UTR) region

114 of the genome by replacing the fragment between restriction sites SpeI and SacII. To generate the

115 complete   5'   UTR   fragment   we   used   PCR   and   the   forward   primer

116 5'GCCACTAGTACGACGGCCAGTGAATTC3';   and   reverse   primer

117   5'CAGCCGCGGATCGATGACCTTACCCACG3', to generate the NS5B-3'UTR region we used

118   forward primer 5'GCCACTAGTAATGTGTCTGTGGCGTTGG3'; reverse primer

119   5'CAGCCGCGGAAACAGCTATGACCATGA3' and the pJ6/JFH-1 RLuc (p7-RLuc2A)

120   plasmid as a template. Each Forward primer has sequence for restriction site, SpeI, and each

121   Reverse primer has sequence for SacII. The control plasmid pRL-TK was obtained from Promega

122   (Madison, USA). A pT7 Fluc containing plasmid, herein called pT7 Fluc (Promega, Madison,

123   USA), was used to generate control mRNA for translation assays.

124

125   **In vitro RNA transcription**

126   To generate full length viral RNA the plasmid pJ6/JFH-1 RLuc (p7-RLuc2A) or related mutants

127   were linearized by digestion with XbaI and RNA was made by using the MEGA Script T7 High

128   Yield Transcription Kit (Life Technologies, Burlington, Canada). The transcription process was

129   performed using the suggested manufacturer's protocol. Fluc mRNA transcript was prepared by

130   digesting the plasmid, pT7 Fluc mRNA, with XmnI and mRNA was prepared using the mMessage

131   mMachine mRNA synthesis kit (Life Technologies, Burlington, Canada) using manufacturer's

132   protocol.

133

134   **Small interfering RNA (siRNA) design and sequence**

135   HCV targeting siRNAs that anneal to regions in IRES, NS5B coding region and 3'UTR were

136   designed using online software, i-score, https://www.med.nagoya-

137   u.ac.jp/neurogenetics/i_Score/i_score.html (31). The sequence of siRNA JFH-1 6367 (si6367) was

138   adapted from the siRNA described previously to inhibit the HCV con1 genotype, by modifying

139   the sequence to match the same region in JFH-1 GACCCACAAACACCAAUUCCC (32). The

6

140   control siRNA (siControl) target sequence is GAGAGUCAGUCAGCUAAUCA and does not

141   anneal to the virus genome. All siRNAs that anneal to the HCV genome were designed to have 21

142   nucleotides; 19 nucleotides complementary to target site and 2 UU overhangs on the 3' end for

143   incorporating into RISC complex, unless stated otherwise (Supplementary Table 3). These siRNAs

144   were synthesized by GE Lifesciences Dharmacon. Anti-miR-122, miRIDIAN microRNA Human

145   hsa-miR-122-5p-Hairpin Inhibitor (IH-300591-06-0050), were purchased from Dharmacon

146   Horizon Discoveries (Chicago, USA).

147

148   **Cell Culture**

149   miR-122 knockout (miR-122 KO) Huh-7.5 (33), Ago2 knockout (Ago2 KO) Huh-7.5 cells (13)

150   and DROSHA/Ago2 KO cells were cultured in Dulbecco's modified Eagle medium (DMEM)

151   supplemented with 10% fetal bovine serum, 0.1 nM non-essential amino acids (Wisent, Montreal,

152   Canada) and 100 ug/ml Pen/Strep (Invitrogen, Burlingtion, Canada). miR-122 knockout Huh-7.5

153   cells were a kind gift from Dr Matthew Evans. DROSHA/Ago2 KO Huh 7.5 cells were generated

154   from DROSHA KO Huh 7.5 cells (34) (a gift from Dr. Charlie Rice) by using the CRISPR-Cas9

155   genome editing techniques (35).

156

157   **siRNA suppression assay**

158   To assess the ability of an siRNA to suppress mRNA translation and assess whether the siRNAs

159   are functional in the RISC, we assessed their impact in a transient suppression assay (Figure 2B).

160   For this assay we used reporter plasmids (pFluc JFH-1 5'UTR / pFuc JFH-1 NS5B-3'UTR) that

161   express Fluc mRNAs containing the siRNA target sequence from HCV in their 3'UTRs. We also

162   used an Rluc expressing control plasmid, pRL-TK to normalize transfection efficiency (Promega,

7

163   Madison, USA). The day before transfection 8 x 10^4 miR-122 KO cells/well were plated in a 24

164   well dish and incubated overnight. The next day, the cells were transfected with 100ng of each of

165   pRL-TK and pFluc JFH-1 (5'UTR or NS5B-3'UTR) and 0.1pmol of a particular test siRNA. The

166   transfection mixture was prepared using 1 µl lipofectamine 2000 according to the suggested

167   manufacture's protocol (Life Technologies, Burlington, Canada). The cells were incubated at

168   37°C, 5% CO2 after transfections and after 48 hours were lysed using passive lysis buffer and

169   assayed for Fluc and Rluc activity using a dual luciferase assay kit (Promega, Madison, USA)

170   (13).

171

172   **HCV replication Assay**

173   Ago2 KO Huh-7.5 cells were co-electroporated as described previously (36) with 5ug J6/JFH-

174   1(p7-Rluc2a) RNA or related point mutant viral RNAs, 60 pmol of test or control siRNAs and 60

175   pmol of anti-miR-122. In all samples in an experiment the amount of small RNAs added per

176   sample was equivalent, and if necessary siControl was added to balance the amount of small

177   RNA (13). Cells were harvested 2 hours, 24 hours, 48 hours and 72 hours post-electroporations

178   and assayed for Rluc expression. HCV replication was assessed based on Rluc expression and

179   was normalized to a positive control sample in which replication of J6/JFH-1(p7-Rluc2a) RNA

180   was supported by endogenous cellular miR-122 (Endo miR-122).

181

182   **Generation of Ago2/ DROSHA knockout Huh-7.5 cells**

183   To generate the double knockout Huh 7.5 cells, we used CRISPR-Cas9 gene editing system to

184   knockout Ago2 in DROSHA knockout Huh 7.5 cells provided to us by Dr. Charlie Rice (34).

185   Three   synthetic   guide   RNAs   (AAUACCUGUUAACUCUCCUC-140585131;

186   UAAUUUGAUUGUUCUCCCGG-140585231, GGCGCAGGAGGUGCAAGUGC-140585310)

187   were designed using the Synthego knockout design tool (https://design.synthego.com/#/) in such

188   a way that the guide RNAs would result in a frameshift deletion in the early region of the exon 2

189   in the Ago2 gene. DROSHA knockout cells were transfected with the TrueCut™ Cas9 Protein v2

190   (Invitrogen, Thermo Fisher Scientific, Vilnius, Lithuania) and the guide RNAs (Synthego

191   CRISPRevolution EZkit, Redwood City, USA) using the Lipofectamine™ CRISPRMAX™ Cas9

192   Transfection Reagent (Invitrogen, Thermo Fisher Scientific, Carlsbad, USA) according to the

193   manufacturer's protocol (Quick Reference: Invitrogen, Thermo Fisher Scientific, Lipofectamine

194   CRISPRMAX Transfection Reagent Pub. No.: MAN0014545). 48 hours post transfection, the

195   cells were passaged, and a portion of the cells collected to test the knockout efficiency. Knockout

196   efficiency was assessed by sanger sequencing of a PCR product that amplified the Crispr targeted

197   region of the Ago2 gene, generated using primers- forward:

198   5'ATTCATGCTGCCTCATCTCTCC3' and reverse: 5'CGGAAGAAGGTATGAGGCAA3'.

199   PCR was performed using the PfuUltra II Fusion High-fidelity DNA polymerase (Agilent,

200   California, USA) using genomic template DNA extracted using QuickExtract DNA extraction

201   solution (Epicentre/ Lucigen, Wisconsin, USA). DNA was prepared by harvesting the cells in the

202   QuickExtract DNA extraction solution and heating the samples at 65⁰C for 15 min, 68⁰C for 15

203   min and 98⁰C for 10 min. The ABI file obtained after sanger sequencing was examined for indels

204   on the Synthego ICE tool (https://ice.synthego.com/#/) and the knockout efficiency was found to

205   be 90%. An array dilution method was used to isolate single cell colonies and condition media was

206   used to encourage the growth of the single clones. Condition medium was obtained by collecting

207   the medium used for growing the knockout pool of cells, filtered using a 0.22µm filter and stored

208   at -20⁰C prior to use. Successful knockout of both Ago2 alleles in the DROSHA knockout cells

209 was identified based on analysis for the loss of siRNA knockdown phenotype based on HCV

210 replication promotion by 5' UTR annealing siRNAs and confirmed by western blot and genome

211 sequencing.

212

213 **Phenotypic analysis of DROSHA/Ago2 knockout cells**

214 To confirm knockout of Ago2 in the DROSHA/Ago2 KO cells we assessed the ability of the cells

215 to support HCV replication promotion by si18-36, as compared to DROSHA KO wild type cells

216 in which the siRNA will knock-down and thus fail to promote HCV (Figure 8A). Isolated clones

217 of putative DROSHA/Ago2 double knockout cells were seeded in 24-well plate 24 hours prior to

218 transfection with 1 ug of J6/ JFH-1(p7-Rluc2a) RNA and 12 pmol small RNAs. miR-122 was used

219 as positive control and siControl was used as negative control. Transfections were performed using

220 Lipofectamine 2000 (Invitrogen, Carlsbad, USA) as per manufacturer's protocol. Cells were

221 harvested 48 hours post transfection and Rluc expression was measured.

222

223 **Western blot**

224 Knockout of Ago2 was confirmed by western blot analysis for the expression of Ago2 (Figure

225 8B), (Supplementary Figure 2C). Putative DROSHA/Ago2 knockout cells were treated with 1x

226 SDS lysis buffer (with 1% 1M DTT) and heated at 95ºC for 5min. The proteins were then separated

227 using a 7.5% SDS-PAGE gel and transferred to a nitrocellulose membrane (GE healthcare

228 Lifesciences, Amersham Protran 0.45 NC membranes, Freiburg, Germany). The membrane was

229 blocked with 5% skimmed milk (BD Difco) and probed with 1:1000 diluted primary anti-Ago2 rat

230 monoclonal antibody clone 11A9 (Millipore Sigma/ Merck KGaA MABE 253, Darmstadt,

231 Germany), 1:25000 diluted primary mouse monoclonal anti-beta actin antibody (AC-15) (Abcam

232   ab6276, Cambridge, USA) and subsequently with 1:40000 diluted secondary peroxidase

233   conjugated AffiniPure Goat Anti-Rat IgG (H+L) (Jackson Immunoresearch 112-035-003, West

234   Grove, USA) and 1: 25000 diluted secondary HRP conjugated Goat anti-mouse IgG (H+L)

235   (BioRad, Mississauga, Canada). The blot was developed using Clarity Western ECL substrate

236   (BioRad, Mississauga, Canada) and imaged with BioRad ChemiDoc MP Imaging system.

237

238   **HCV translation assay**

239   To assess siRNA promotion of HCV translation, DROSHA/Ago2 KO Huh-7.5 cells were co-

240   electroporated with 5ug of non-replicative mutant HCV genomic RNA, J6/JFH-1(p7-Rluc2a)

241   GNN, 1ug of control T7 Fluc mRNA, and 60 pmol of test siRNA. As positive control J6/JFH-

242   1(p7-Rluc2a) GNN was electroporated with miR-122, since the DROSHA/Ago2 KO Huh-7.5

243   cells lack miR-122 expression. As a negative control, J6/JFH-1(p7-Rluc2a) GNN was

244   electroporated with siControl. Cells were harvested 4 hours post-electroporations and assayed for

245   Rluc and Fluc expression.

246

247   **Luciferase assay**

248   Luciferase expression was measured by using Firefly, *Renilla*, or Dual luciferase kits (Promega,

249   Madison, USA) as suggested by the manufacturer's protocols. Cells were washed once in

250   Dulbecco's phosphate-buffered saline then lysed with 100 ul of passive lysis buffer. 10 ul of the

251   cell extract was mixed with the appropriate luciferase assay substrate and light emission was

252   measured by using a Glomax 20/20 Luminometer (Promega, Madison, USA).

253

254   **RNA purification**

255   Cells were harvested into 1 ml of Trizol and total cellular RNA was isolated using the

256   manufacturer's provided protocol (Life Technologies, Burlington, Canada).

257

258   **HCV genome stabilization assay and northern blots**

259   To assess the impact of miR-122 and the siRNAs on HCV genome stability we assessed the amount

260   of non-replicative HCV RNA present in cells at various times post-electroporation using northern

261   blot analysis (Figure 9), (Supplementary Figure 2A and B). For each assay, 32×10^6

262   DROSHA/Ago2 knockout Huh-7.5 cells were electroporated (in 4 cuvettes) with 40 μg of HCV

263   J6/JFH-1(p7-Rluc2a) GNN RNA and 240 pmol of one of the small RNAs (si15-33, si19-37, si26-

264   44, or si27-45) or miR-122 (as a positive control) or siControl (as a negative control). Cells from

265   the 4 electroporation cuvettes were pooled and plated onto four 10 cm plates. Cells for the 0 min

266   time point were harvested immediately after electroporation, and the others were incubated at 37°C

267   and harvested at 30 mins, 60 mins and 120 mins post-electroporation. Total cellular RNA was

268   harvested using Trizol as recommended by the manufacturer (Life Technologies, Burlington,

269   Canada), and 10 ug were separated on an 0.8% agarose gel and transferred to a Nylon membrane

270   (GE Healthcare Limited, Buckinghamshire, England) as described previously (36). The transferred

271   RNAs were crosslinked to the membrane using a UV crosslinker (Spectrolinker XL-1000) at X100

272    $\mu J/cm^2$ for 12 seconds and cut in half to probe for HCV RNA and GAPDH separately. The

273   radioactive DNA probes used were prepared using Prime-a-Gene Labeling System kit (U1100,

274   Promega, Madison, WI, USA), and radiolabeled dCTP (PerkinElmer, Boston, USA). The probes

275   were generated from a 3 kbp BamHI-to-EcoRV DNA fragment of the pJ6/JFH-1 RLuc (p7-

276   RLuc2A) plasmid or a 1.3 kb cDNA fragment of human GAPDH. Radioactive bands were detected

277   by exposing the membranes overnight on a phosphorscreen and scanned using a Phosphoimager

278   (Typhoon, GE Healthcare Life Sciences, Mississauga, Canada). Band signal intensities were

279   quantified using Image Studio Lite version 5.2.5.

280

281   **RNA structure prediction analysis**

282   RNA structure predictions were done using the RNA prediction software 'RNA structure'

283   available from the website by the Matthews lab at https://rna.urmc.rochester.edu/index.html. (37).

284   Single RNA structure predictions were performed using algorithm 'fold' and structure predictions

285   of two interacting RNA molecule were predicted using algorithm 'bifold'. Dot-bracket files for

286   the five lowest free energy structures were generated using the RNA fold command in

287   'RNAstructure' and RNA images were generated from them using VARNA (VARNA GUI applet)

288   (38).

289

290   **Statistical analysis**

291   All data are displayed as the mean of three or more independent experiments, and error bars

292   indicate standard deviation of the mean. Where appropriate, one-way ANOVA was performed

293   using Graph Pad Prism version 8.3 for MacOS (San Diego, USA, www.graphpad.com). In graphs,

294   statistical significance is indicated as follows: *$P<0.0332$; **$P< 0.0021$; ***$P < 0.0002$; ****$P <$

295   0.0001.

296

297   **RESULTS:**

298

299   **siRNA annealing to nucleotides between 15 to 44 on 5'UTR promotes virus replication.**

300   Annealing of miR-122 to two complementary sequences on 5'UTR of the HCV genome is required

301   for detectible HCV replication in cell culture (27, 39). In our previous work we showed that HCV

302   replication was promoted efficiently by 5' UTR targeting siRNAs when siRNA directed cleavage

303   activity was abolished by using Ago2 knockout cells (Ago2 KO) (13). Thus, replication promotion

304   does not require the specific annealing pattern generated by miR-122 or binding of two small RNA

305   copies, but we hypothesized that it may be impacted by the annealing location. To test this

306   hypothesis, we determined the range of genome locations to which small RNA annealing can

307   promote HCV replication. First, we designed and tested an array of siRNAs with target sequences

308   that walk the 5'UTR between nucleotides 10 to 47 at single nucleotide resolution (Figure 2A).

309   Each siRNA was 19 nucleotides long and contained two 3' UU (uracil) overhangs to ensure RISC

310   loading (Supplementary Table 3). The siRNAs were named based on the 19 nucleotide positions

311   on the HCV genome to which they bind, from si10-28 to si29-47 (Figure 2A). To confirm RISC

312   loading, the siRNAs were tested for their ability to knockdown gene expression in a suppression

313   assay (Figure 2B). For suppression assays, we transfected cells with a plasmid, pFluc JFH-1

314   5'UTR, that expresses an mRNA encoding Fluc having the HCV miR-122 binding region/siRNA

315   target sites in its 3' UTR. This plasmid was co-transfected in miR-122 KO Huh 7.5 cells (cells that

316   express Ago2), with a test siRNA and knockdown was measured based on Fluc expression

317   compared to cells transfected with a control siRNA (siControl). Fluc expression levels were

318   assessed relative to Rluc expression from a transfection control plasmid, pRL-TK. We observed

319   that siRNAs binding from nucleotides 14 onwards were significantly (p value <0.0001) able to

320   suppress Fluc expression at different levels compared to siControl, implying that they were

321   actively incorporated into the RISC complex (Figure 2C) (Supplementary Table 1). Most siRNAs

322   that bound within SLI did not knockdown Fluc and thus did not enter RISC, likely due to the

14

323   hairpin structure formation. Inactive siRNAs were omitted from further analyses. After confirming

324   RISC incorporation, we determined the ability of the siRNAs to promote HCV replication in

325   replication assays. For these assays we electroporated Ago2 KO Huh 7.5 cells with J6/JFH-1(p7-

326   Rluc2a) RNA, anti-miR-122, an antagonist of endogenous miR-122, and a test siRNA, and HCV

327   replication was assessed 2 hours, 24 hours, 48 hours and 72 hours post-electroporation based on

328   luciferase expression as a proxy for HCV replication (Figure 2D). We electroporated J6/JFH-1(p7-

329   Rluc2a) RNA without anti-miR-122 as a positive control to measure HCV RNA replication

330   induced by endogenous miR-122 (Endo miR-122). RLuc expression in this sample at 72 hours

331   post-electroporation was deemed 100% and used to calculate relative luciferase levels in the rest

332   of the samples. The negative controls (siControl) (Figure 2D) containing viral RNA, anti-miR-122

333   and siControl (an HCV non-targeting siRNA) confirmed abolition of HCV replication by the miR-

334   122 antagonist. In other samples the addition of indicated siRNA reinstated HCV replication to

335   the relative levels shown (Figure 2D), (Supplementary Table 1). An siRNA that anneals within the

336   NS5B coding sequence (si6467) did not promote HCV replication but siRNAs binding between

337   nucleotides 15 and 44 did. HCV replication was promoted most efficiently by si19-37 and was

338   similar to replication induced by endogenous miR-122 (Endo miR-122), and less efficient

339   replication induction was observed using siRNAs that annealed to locations moving away from

340   nucleotides 19-37 in either direction (Figure 2D and F). The 5' boundary to which siRNAs can

341   promote HCV was nucleotide 15. Si14-32 did not promote detectable HCV replication and siRNAs

342   that anneal nearer to the 5' UTR did not enter RISC and thus could not be tested (Figure 2C). The

343   3' boundary of the region to which siRNA annealing promoted HCV RNA was nucleotide 44 and

344   si26-44 was the last siRNA to promote virus replication (p value <0.0001). si26-44 promoted HCV

345   replication; however, si27-45 and those that bound further in the 3' direction did not. Thus, either

15

346   annealing to nucleotide 26 was essential for promotion, or siRNA annealing to nucleotide 45 and

347   onwards was detrimental. To distinguish between these possibilities, we designed two additional

348   siRNAs, si26-45 and si27-44. Both siRNAs were active in suppression assays, however only si27-

349   44 promoted HCV replication (Figure 2E), (Supplementary Table 1). This indicated that annealing

350   to nucleotide 45, inhibited promotion activity and annealing to nucleotide 26 is not essential

351   (Figure 2E). Thus, we have defined the 3' boundary of the region to which small RNA annealing

352   can promote HCV replication as nucleotide 44.

353

354   **siRNA annealing to the HCV IRES do not promote or inhibit HCV replication.**

355   To determine whether siRNAs binding on other regions of HCV genome can promote virus

356   replication, we designed siRNAs using online software, i-score, to determine best target sites

357   within the HCV IRES region (31). We designed 6 siRNAs that bind to various sites on the IRES

358   regions namely si38-56, si42-60, si73-91, si88-106, si317-338 and si339-357 (Figure 3A). We

359   validated the knockdown activity of these siRNAs to confirm their incorporation into RISC, and,

360   5 out of 6 showed suppression activity (Supplementary Figure 1A). However, none of the active

361   siRNAs promoted replication in HCV replication assays (Figure 3B).

362   Small RNAs that anneal within the IRES and downstream of nucleotides 45, and thus

363   within SLII of the IRES did not promote detectable HCV replication. We hypothesized that these

364   siRNAs may have failed to promote HCV because they anneal to, and interfere with the activity

365   of the IRES and thus inhibit HCV replication. To test this hypothesis, we assessed inhibition of

366   HCV by the IRES targeting siRNAs. For these assays we used a mutant HCV RNA, U25C, that

367   can replicate independent from miR-122, and thus replicated in Ago2 knockout cells even when

368   miR-122 is antagonized. This assay was used instead of miR-122-promoted replication to

16

369 eliminate the possible influence of annealing competition between miR-122 and the siRNAs tested.

370 Using this assay, we observed no HCV replication promotion or inhibition by the IRES-binding

371 siRNAs, while replication was promoted by the positive control siRNA, si19-37 (Figure 3C). Thus,

372 our data suggests that IRES-binding siRNAs do not promote or inhibit HCV replication.

373

374 **siRNA annealing to the alternative predicted miR-122 binding sites do not promote HCV**

375 **replication.**

376 Other potential miR-122 binding sites have been reported in the NS5B coding region and

377 the 3'UTR region of HCV genome (40–43). We therefore also assessed whether siRNAs binding

378 on any of these potential miR-122 binding sites affected HCV replication (Figure 4). We started

379 by designing siRNAs binding to 7 predicted miR-122 binding sites in NS5B and 3'UTR region.

380 For convenience we named these siRNAs according to the region they bind and in serial order,

381 namely siNS5B1, siNS5B2, siNS5B3, siNS5B4, si3'UTR1, si3'UTR2 and si3'UTR3 (Figure 4A

382 and B). In order to test these in our suppression assay, we replaced the 5'UTR with NS5B-3'UTR

383 regions in suppression plasmid to have target sites for our siRNAs. We observed that each of seven

384 siRNAs were able to suppress Fluc expression suggesting they all entered RISC (Supplementary

385 Figure 1B). To assess their role in HCV replication, we performed HCV replication assays and

386 observed that Rluc expression after addition of the NS5B and 3' UTR targeting siRNAs was

387 comparable to the negative controls (siControl and si6367) (Figure 4C). Thus, siRNA binding to

388 other predicted miR-122 binding sites did not promote virus replication. Overall our data show

389 that small RNAs that bind between nucleotides 15-44 on the HCV 5' UTR promote HCV

390 replication.

391

17

392   **Small RNAs that promote virus replication are predicted to induce the canonical 5' UTR**

393   **RNA structure**

394   We and others hypothesized that the pro-viral activity of miR-122 was mediated by

395   annealing induced RNA structural changes to the HCV 5' UTR that promote the formation of the

396   canonical 5' UTR IRES (Figure 1 A and B) (12, 13, 24). In the presence of miR-122 the HCV 5'

397   terminal 117 nucleotides were predicted to form SLIIa and SLIIb, essential IRES elements, and

398   SLI, an essential replication element (Figure 1A and C). However, in the absence of miR-122, the

399   5' UTR RNA is predicted to form SLI and an alternative structure instead of SLII and thereby

400   would fail to form an active HCV IRES (Figure 1B). Since siRNAs annealing to different locations

401   promoted virus replication with different efficiencies, we speculated that replication promotion

402   may correspond with the ability of an siRNA to induce the canonical HCV 5' UTR RNA structure.

403   To test this, we used an online RNA secondary structure prediction tool, 'RNAstructure' to predict

404   the structure of the 5' 117 nucleotides of the HCV genome induced by annealing of siRNAs that

405   promote efficient, intermediate, or no HCV replication. The first six lowest delta free energy

406   predicted structures induced by annealing of each siRNAs are shown in Figure 5. We observed

407   that siRNAs that promote efficient virus replication, si17-35, si19-37, si22-42 and si24-42 were

408   predicted to induce the canonical HCV structure one or many times of the six predicted structures

409   (Figure 5), (Supplementary Tables 1 and 2). We also found that the canonical structure was

410   induced by annealing of si26-44 and si27-44 which mark the boundary for replication promotion.

411   However, the canonical structure was not observed with siRNAs si26-45 and si27-45, and whose

412   annealing did not promote HCV replication. This was also observed for si14-32, which did not

413   promote virus replication and was predicted to form an additional non-canonical loop near SLIIa

414   (Figure 5, si14-32, Structure no. 4), and si28-46 which induced a structure in which a stem of SLIIa

18

415   was absent (Figure 5), (Supplementary Table 2). Si15-33 showed intermediate replication

416   promotion and also failed to induce SLI (Figure 5), (Supplementary Table 2). Thus, this data

417   suggests that formation of the complete canonical 5' terminal RNA structure, including SLI, SLIIa

418   and SLIIb by small RNA annealing is required for optimal HCV replication promotion, and that

419   an incomplete canonical structure impairs viral replication.

420

421   **Binding of siRNAs to 15 nucleotides is a minimum requisite to promote efficient small RNA**

422   **dependent HCV replication**

423   Next we wanted to define the minimum annealing requirements for the pro-viral activity

424   of small RNA annealing (Figure 6). To determine this, we designed siRNA analogues of the most

425   efficient siRNA, si19-37, but having sequence matches ranging from 7 to 17 nucleotides on the 3'

426   or 5' ends (Figure 6A). For example: si19(21-37) is 19 nucleotides long with 17 nucleotides (21-

427   37) matching the HCV 5' UTR (Figure 6A). Similarly, si19(23-37), si19(25-37), si19(27-37),

428   si19(27-37), si19(29-37) and si19(31-37) have between 15 and 7 matching nucleotides. si19(21-

429   37), si19(23-37) promoted HCV replication as efficiently as si19-37 and the others did not promote

430   at all (Figure 6B). From the 3' end we generated siRNAs with sequence matches of 16, si19(19-

431   35), 14, si19(19-33), and 12, si19(19-31) matches (Figure 6A) and only si19(19-35) promoted

432   HCV replication (Figure 6C). Suppression assay of all si19-37 analogs showed that siRNA

433   knockdown activity decreased with fewer annealing nucleotides; however, those that promoted

434   replication were all active (Supplementary Figure 1C and D). Thus, with this we can conclude that

435   an siRNA must anneal to at least 15 nucleotides of the HCV 5' UTR to promote efficient

436   replication. RNA structures induced by annealing of these siRNAs resembled the canonical

437   structure, but delta free energy data suggest that the structures may be less stable (Figure 6D).

438   Therefore, our data suggests that location specific siRNA must anneal with a minimum of 15

439   nucleotides to induce the canonical structure and promote efficient virus replication.

440

441   **siRNAs binding to 5' terminus (nts 1-3) enhances HCV replication, but the generation of a**

442   **small RNA overhang does not.**

443   Previous reports showed that replication promotion by miR-122 was enhanced by

444   annealing of miR-122 to nucleotides on the 5' terminus of HCV and by the generation of a 3'

445   overhang (20). To assess the impact of siRNA binding to the 5' terminus (nucleotides 1-3) we

446   compared HCV replication promotion by a small RNA that binds to the 5' terminus with one that

447   does not (Figure 7). We designed an siRNA, si1-3--21-36, that binds to 21-36 and to the 5' terminal

448   3 nucleotides and found that it promoted replication about 4 fold more efficiently than si1-3mm--

449   21-36, that also binds to nts 21-36 but not the 5' terminus (Figure 7A and B). Both siRNAs were

450   active in our suppression assays (Supplementary Figure 1E). Indeed, HCV replication promoted

451   by si1-3--21-36 was around 2-fold higher than the most efficient siRNA, si19-37, identified in

452   Figure 2D. Further, the canonical 5' UTR RNA structure was induced regardless of 5' end

453   annealing. This supports that end annealing is not required for pro-viral siRNA annealing but

454   suggests that it has a positive effect on virus replication (Figure 7C).

455   The annealing of miR-122 to binding site 1 on the HCV genome generates a 7-nucleotide

456   overhang of the HCV 5' terminus that was reported to contribute to the efficiency of replication of

457   HCV with miR-122 (20). Since the siRNAs used in this study only consisted of 2 UU overhangs,

458   we knew that a long miR-122 like overhang was not essential for replication promotion, but we

459   wanted to test if having such an overhang contributes to replication. To test this, we assessed

460   replication promotion by an siRNA that has a miR-122-like overhang, 'si mir ovh1-3--21-36', with

461   one that does not, 'si no ovh1-3--21-36' (Figure 7D). Both siRNAs were active in our suppression

462   assays (Supplementary Figure 1E). Further, both siRNAs are predicted to induce formation of

463   canonical predicted HCV structures (Figure 7F) but we found that the miR-122-like overhang did

464   not enhance replication promotion, and in fact, decreased HCV replication efficiency (Figure 7E).

465   This experiment confirmed that generation of a 5' overhang is not required for and may hinder

466   HCV replication.

467

468   **siRNA promotion of virus replication correlates with promotion of virus translation**

469   Two confirmed functions of miR-122 are promotion of HCV translation and stabilization

470   of the viral genome, however, the relative contributions of each to HCV life-cycle promotion are

471   unknown (27, 39, 44). We hypothesized that if stimulation of translation or genome stabilization

472   is a key mechanism by which miR-122 promotes virus replication then the ability of an siRNA to

473   promote replication will correlate with its ability to stimulate translation or stabilize the viral

474   genome. To test this hypothesis, we assessed siRNA stimulation of translation and genome

475   stabilization by panels of siRNAs that promote HCV with varying efficiencies.

476   To assess siRNA translation promotion, we measured the ability of miR-122 and an array

477   of siRNAs to promote translation of a non-replicative HCV J6/JFH-1(Rluc2a) GNN RNA in

478   DROSHA/Ago2 double KO cells. DROSHA/Ago2 double KO cells were generated to provide a

479   background that lacked both miR-122 expression and Ago2 associated siRNA cleavage activity

480   and allowed us to remove the miR-122 antagonist from our assays. DROSHA/Ago2 double KO

481   cells were generated from DROSHA knockout cells using Crispr/Cas9 and the knockout of Ago2

482   was confirmed based on the ability of the cells to use si18-36 to promote instead of knockdown

483   HCV replication (Figure 8A) and by western blot analysis showing abolished Ago2 expression.

484   (Figure 8B), (Supplementary Figure 2C). To assess HCV translation promotion by the siRNAs,

485   cells were electroporated with viral RNA and siRNAs and translation efficiency was measured

486   based on Rluc expression vs a co-electroporated Fluc mRNA control (Figure 8C). By using an

487   array of siRNAs that promote replication with different efficiencies we found that the levels of

488   translation stimulation correlated with their ability to promote replication (Figure 8C and D),

489   (Supplementary Table 1). siRNAs that promoted efficient HCV replication, si17-35, si18-36, si19-

490   37, si22-40, and si24-42 also efficiently stimulated translation, and siRNAs that promoted HCV

491   replication to a moderate level also promoted translation less efficiently. Finally, siRNAs that

492   promoted HCV replication poorly displayed little or no translation stimulation (Figure 8C and D)

493   (Supplementary Table 1). Our data thus suggests that translation stimulation is linked with small

494   RNA promotion of HCV translation and supports the hypothesis that a primary mechanism of

495   miR-122 promotion of HCV is by stimulating translation by inducing the formation of the HCV

496   IRES.

497

498   **siRNA annealing-induced HCV genome stabilization is not sufficient to promote virus**

499   **replication**

500   In addition to stimulating HCV translation, miR-122 annealing also stabilizes the HCV

501   genomic RNA by protecting it from cellular pyrophosphatases, Dom3Z and Dusp11, and the

502   exonuclease Xrn1 (23). To test for a linkage between siRNA induced replication and virus genome

503   stabilization we investigated HCV RNA genome stability in presence of miR-122, and four

504   different siRNAs (Figure 9) (Supplementary Figure 2A and B). We chose si19-37 because it

505   promotes efficient replication, two siRNAs, si15-33 and si26-44 that promote intermediate levels

506   of replication, and one siRNA, si27-45 that does not promote replication. miR-122 was used as a

507   positive control and siControl was used as a negative control. For the stability assays HCV J6/JFH-

508   1(p7-Rluc2a) GNN RNA, a non-replicative HCV RNA and an siRNA (or miR-122, or control)

509   were electroporated in DROSHA/Ago2 double KO cells and total RNA was harvested at 0min, 30

510   mins, 60 mins and 120 mins post-electroporation. To determine the half-life of HCV GNN RNA

511   northern blots were performed (Figure 9). As expected, the half-life of the viral RNAs was

512   extended by miR-122 annealing (Figure 9A), however, contrary to our expectations all siRNA

513   stabilized the HCV genome, regardless of whether they promoted HCV replication or not (Figure

514   9, si27-45) (Supplementary Table 1). Further, no correlation between half-lives and the levels of

515   RNA replication was observed (Figure 9A and B). This suggests that although small RNAs may

516   stabilize the HCV genomic RNA this is not sufficient to promote HCV genome replication. Thus,

517   stimulation of translation appears to be the essential role of miR-122 annealing in promotion of

518   HCV replication, and genome stabilization, while stimulatory, is not sufficient alone.

519

520   **DISCUSSION:**

521   miR-122 binding to two sites on HCV 5'UTR is required for efficient HCV replication

522   (Figure 2A). We previously reported a hypothesis that the pro-viral activity of miR-122 was

523   mediated by annealing induced RNA structural changes to the HCV 5' UTR to induce the

524   formation of the canonical 5' UTR IRES structure (13). We also showed that HCV replication was

525   stimulated by siRNAs as efficiently as by miR-122 if their siRNA-directed cleavage activity was

526   abolished by using Ago2 KO cells (13). In this study we have defined the locations on the HCV

527   genome to which small RNA annealing induces HCV replication further defined the underlying

528   mechanism of replication promotion by miR-122. We identified that small RNA annealing to

529   nucleotides 1-3 and 15 - 44 promote HCV replication and that annealing to nucleotide 45 (SLIIa)

23

530 and beyond do not (Figure 1 and 7). Further siRNAs binding to 15 nucleotides is required (Figures

531 6). We found that the ability of siRNAs to promote replication is related to their ability to induce

532 the canonical 5' UTR RNA structure, including formation of SLI, SLIIa, and SLIIb (Figure 5),

533 (Supplementary Tables 1 and 2). This suggests that location specific binding of small RNAs

534 promotes virus replication by favoring the formation of the correct 5' UTR and IRES RNA

535 structures.

536 We also determined that siRNA binding to other regions on HCV genome, including the

537 HCV IRES does not stimulate virus replication. In addition, IRES annealing siRNAs neither

538 promoted nor inhibited HCV replication (Figure 3C) and thus do not appear to disrupt IRES

539 structure and function. Therefore, small RNA annealing induced RNA structure changes appear to

540 be specific to the HCV 5' terminal region and the HCV IRES structures may be too stable to be

541 disrupted by small RNA annealing.

542 At least 7 more miR-122 binding sites were predicted in the HCV genome and were

543 speculated to also affect the virus life cycle, (11, 40, 41, 43). However, none of the siRNAs that

544 bound to the predicted miR-122 binding sites promoted replication (Figure 4). Our data therefore

545 suggests that the two miR-122 binding sites on HCV 5'UTR are the only active binding sites that

546 promote HCV replication. This data is in agreement with a recently published report in which

547 mutation of the other miR-122 binding sites had no influence on HCV replication (40).

548 The minimum annealing required for efficient small RNA induced HCV replication

549 promotion was 15 nucleotides. (Figure 6A and B). This data may explain why annealing of two

550 copies of miR-122 is required for efficient HCV replication since annealing of one copy does not

551 fulfill this requirement but annealing of two copies does (Figure 1). Further, the most efficient

552 HCV promoting small RNA identified in our siRNA walk (si19-37) anneals to nucleotides

553   comprising miR-122 binding seed site 1 (nucleotides 21-27) and the accessory miR-122 binding

554   site 2 (nucleotides 29-31) and suggests that binding to miR-122 binding seed site 1 and accessory

555   site 2 may be the minimum requirement for efficient small RNA dependent HCV replication. This

556   data also supports a previous finding that miR-122 site 1 behaves similar to a conventional

557   miRNA:target interaction where binding to a seed site is important (45), and that miR-122 binding

558   site 2 has higher affinity owing to extended base pairing to the accessory site.

559   A previous report showed that miR-122 binding to the extreme 5' terminus of HCV

560   genome was required for efficient HCV replication (20). Our data indicates that small RNA

561   annealing to the 5' terminal region is not essential but enhances HCV replication promotion

562   (Figure 7A and B). Our structure predictions also showed that siRNAs that interacted with 5'

563   terminal nucleotide induce the canonical IRES structure (Figure 7C). We therefore speculate that

564   small RNA binding to terminal nucleotides on HCV genome may induce the canonical HCV

565   structure better than those that do not. The previous report also showed that the 7 nucleotide 3'miR-

566   122 overhang contributes to virus replication (20). However, our study indicates that a 2UU

567   overhang was sufficient to promote HCV replication, and that generation of a miR-122-like 3'

568   overhang was not necessary and, in fact, was detrimental to HCV replication (Figure 7D and E).

569   All small RNAs that promote HCV replication were predicted to induce the canonical HCV

570   IRES structure (Figure 2D and 5), (Supplementary Table 1). We therefore hypothesized that the

571   ability of a small RNA to induce the IRES and thus stimulate translation will correlate with its

572   ability to promote virus replication. Our data support this hypothesis and showed that siRNAs that

573   promote replication efficiently also stimulated translation efficiently, and that translation

574   stimulation correlated with virus replication levels (Figure 8C and D), (Supplementary Table 1).

575   This suggests that translation stimulation as a key mechanism by which small RNA annealing

576   promotes HCV replication. This data suggests that the miR-122 binding sites might be considered

577   part of the IRES, or an IRES modulator.

578   Annealing of miR-122 to the HCV 5' UTR stabilizes the viral genome, and this has been

579   proposed as a mechanism by which miR-122 promotes HCV replication (13, 25). Further, it was

580   speculated that the mechanism of protection is based on the generation of a double stranded 5'

581   terminus by miR-122 binding which protect it from cellular pyrophosphatases and exonuclease

582   (Figure 2A) (20). We showed previously that si19-37 also stabilized HCV RNA suggesting that

583   small RNAs may also promote virus life cycle by stabilizing the genome. However, si19-37 does

584   not bind to the extreme 5' terminus thus indicating that end annealing and the generation of an

585   overhang is not required for genome stabilization. Further, we show that siRNAs annealing

586   stabilizes the HCV genome regardless of whether they promote replication (Figure 9). Therefore,

587   genome stabilization is not sufficient alone to promote virus replication, but functions to enhance

588   replication induced by translation stimulation.

589   Based on our findings we present a model in which position-specific annealing of small

590   RNAs induces the formation of the viral IRES RNA structures and stimulates virus translation. In

591   addition, position-independent small RNA annealing stabilizes the viral genome but alone is

592   insufficient to promote the virus life cycle (Figure 10). However, it is still unknown whether HCV

593   genome structure changes induced by small RNA binding are fixed throughout the virus lifecycle

594   or whether they are dynamic and differ during specific events in the virus lifecycle such as

595   replication and virion assembly. In addition, the roles of miRNA associated proteins like Ago and

596   Ago complexes in HCV promotion by miR-122 remain to be clarified.

597

598   **FUNDING:**

26

611

612   **REFERENCES:**

613   1. Rijnbrand,R., Bredenbeek,P.J., Haasnoot,P.C., Kieft,J.S., Spaan,W.J. and Lemon,S.M.
614   (2001) The influence of downstream protein-coding sequence on internal ribosome entry
615   on hepatitis C virus and other flavivirus RNAs. *RNA*, **7**, 585–597.

616   2. Perz,J.F., Armstrong,G.L., Farrington,L.A., Hutin,Y.J.F. and Bell,B.P. (2006) The
617   contributions of hepatitis B virus and hepatitis C virus infections to cirrhosis and primary
618   liver cancer worldwide. *J. Hepatol.*, **45**, 529–538.

619   3. Dustin,L.B. (2017) Innate and Adaptive Immune Responses in Chronic HCV Infection.
620   *Curr. Drug Targets*, **18**, 826–843.

621   4. Sagan,S.M., Chahal,J. and Sarnow,P. (2015) cis-Acting RNA elements in the hepatitis C
622   virus RNA genome. *Virus Res.*, **206**, 90–98.

623   5. Johnson,A.G., Grosely,R., Petrov,A.N. and Puglisi,J.D. (2017) Dynamics of IRES-
624   mediated translation. *Philos. Trans. R. Soc. B Biol. Sci.*, **372**, 20160177.

625   6. Fraser,C.S. and Doudna,J.A. (2007) Structural and mechanistic insights into hepatitis C
626   viral translation initiation. *Nat. Rev. Microbiol.*, **5**, 29–38.

27

627   7. Spahn,C.M.T., Kieft,J.S., Grassucci,R.A., Penczek,P.A., Zhou,K., Doudna,J.A. and
628   Frank,J. (2001) Hepatitis C Virus IRES RNA-Induced Changes in the Conformation of the
629   40S Ribosomal Subunit. *Science*, **291**, 1959–1962.

630   8. Lukavsky,P.J., Kim,I., Otto,G.A. and Puglisi,J.D. (2003) Structure of HCV IRES domain
631   II determined by NMR. *Nat. Struct. Mol. Biol.*, **10**, 1033–1038.

632   9. Paulsen,R.B., Seth,P.P., Swayze,E.E., Griffey,R.H., Skalicky,J.J., Cheatham,T.E. and
633   Davis,D.R. (2010) Inhibitor-induced structural change in the HCV IRES domain IIa RNA.
634   *Proc. Natl. Acad. Sci.*, **107**, 7263–7268.

635   10. Jopling,C.L., Yi,M., Lancaster,A.M., Lemon,S.M. and Sarnow,P. (2005) Modulation of
636   Hepatitis C Virus RNA Abundance by a Liver-Specific MicroRNA. *Science*, **309**, 1577–
637   1581.

638   11. Jopling,C.L., Schütz,S. and Sarnow,P. (2008) Position-Dependent Function for a Tandem
639   MicroRNA miR-122-Binding Site Located in the Hepatitis C Virus RNA Genome. *Cell
640   Host Microbe*, **4**, 77–85.

641   12. Schult,P., Roth,H., Adams,R.L., Mas,C., Imbert,L., Orlik,C., Ruggieri,A., Pyle,A.M. and
642   Lohmann,V. (2018) microRNA-122 amplifies hepatitis C virus translation by shaping the
643   structure of the internal ribosomal entry site. *Nat. Commun.*, **9**, 2613.

644   13. Amador-Cañizares,Y., Panigrahi,M., Huys,A., Kunden,R.D., Adams,H.M., Schinold,M.J.
645   and Wilson,J.A. (2018) miR-122, small RNA annealing and sequence mutations alter the
646   predicted structure of the Hepatitis C virus 5′ UTR RNA to stabilize and promote viral
647   RNA accumulation. *Nucleic Acids Res.*, **46**, 9776–9792.

648   14. Israelow,B., Mullokandov,G., Agudo,J., Sourisseau,M., Bashir,A., Maldonado,A.Y.,
649   Dar,A.C., Brown,B.D. and Evans,M.J. (2014) Hepatitis C virus genetics affects miR-122
650   requirements and response to miR-122 inhibitors. *Nat. Commun.*, **5**.

651   15. Lee,Y., Jeon,K., Lee,J.-T., Kim,S. and Kim,V.N. (2002) MicroRNA maturation: stepwise
652   processing and subcellular localization. *EMBO J.*, **21**, 4663–4670.

653   16. Lam,J.K.W., Chow,M.Y.T., Zhang,Y. and Leung,S.W.S. (2015) siRNA Versus miRNA
654   as Therapeutics for Gene Silencing. *Mol. Ther. Nucleic Acids*, **4**, e252.

655   17. Hutvágner,G. and Zamore,P.D. (2002) A microRNA in a multiple-turnover RNAi enzyme
656   complex. *Science*, **297**, 2056–2060.

657   18. Brennecke,J., Stark,A., Russell,R.B. and Cohen,S.M. (2005) Principles of MicroRNA–
658   Target Recognition. *PLOS Biol.*, **3**, e85.

659   19. O'Brien,J., Hayder,H., Zayed,Y. and Peng,C. (2018) Overview of MicroRNA Biogenesis,
660   Mechanisms of Actions, and Circulation. *Front. Endocrinol.*, **9**.

661 20. Machlin,E.S., Sarnow,P. and Sagan,S.M. (2011) Masking the 5' terminal nucleotides of
662 the hepatitis C virus genome by an unconventional microRNA-target RNA complex.
663 *Proc. Natl. Acad. Sci.*, **108**, 3193–3198.

664 21. Li,Y., Masaki,T., Yamane,D., McGivern,D.R. and Lemon,S.M. (2013) Competing and
665 noncompeting activities of miR-122 and the 5' exonuclease Xrn1 in regulation of
666 hepatitis C virus replication. *Proc. Natl. Acad. Sci. U. S. A.*, **110**, 1881–1886.

667 22. Shimakami,T., Yamane,D., Jangra,R.K., Kempf,B.J., Spaniel,C., Barton,D.J. and
668 Lemon,S.M. (2012) Stabilization of hepatitis C virus RNA by an Ago2–miR-122
669 complex. *Proc. Natl. Acad. Sci.*, **109**, 941–946.

670 23. Amador-Cañizares,Y., Bernier,A., Wilson,J.A. and Sagan,S.M. (2018) miR-122 does not
671 impact recognition of the HCV genome by innate sensors of RNA but rather protects the
672 5′ end from the cellular pyrophosphatases, DOM3Z and DUSP11. *Nucleic Acids Res.*, **46**,
673 5139–5158.

674 24. Chahal,J., Gebert,L.F.R., Gan,H.H., Camacho,E., Gunsalus,K.C., MacRae,I.J. and
675 Sagan,S.M. (2019) miR-122 and Ago interactions with the HCV genome alter the
676 structure of the viral 5′ terminus. *Nucleic Acids Res.*, **47**, 5307–5324.

677 25. Masaki,T., Arend,K.C., Li,Y., Yamane,D., McGivern,D.R., Kato,T., Wakita,T.,
678 Moorman,N.J. and Lemon,S.M. (2015) miR-122 Stimulates Hepatitis C Virus RNA
679 Synthesis by Altering the Balance of Viral RNAs Engaged in Replication versus
680 Translation. *Cell Host Microbe*, **17**, 217–228.

681 26. Fukuhara,T., Kambara,H., Shiokawa,M., Ono,C., Katoh,H., Morita,E., Okuzaki,D.,
682 Maehara,Y., Koike,K. and Matsuura,Y. (2012) Expression of MicroRNA miR-122
683 Facilitates an Efficient Replication in Nonhepatic Cells upon Infection with Hepatitis C
684 Virus. *J. Virol.*, **86**, 7918–7933.

685 27. Wilson,J.A. and Huys,A. (2013) miR-122 Promotion of the hepatitis C virus life cycle:
686 sound in the silence. *WIREs RNA*, **4**, 665–676.

687 28. Meister,G., Landthaler,M., Patkaniowska,A., Dorsett,Y., Teng,G. and Tuschl,T. (2004)
688 Human Argonaute2 Mediates RNA Cleavage Targeted by miRNAs and siRNAs. *Mol.
689 Cell*, **15**, 185–197.

690 29. Carthew,R.W. and Sontheimer,E.J. (2009) Origins and Mechanisms of miRNAs and
691 siRNAs. *Cell*, **136**, 642–655.

692 30. Jones,C.T., Murray,C.L., Eastman,D.K., Tasello,J. and Rice,C.M. (2007) Hepatitis C
693 Virus p7 and NS2 Proteins Are Essential for Production of Infectious Virus. *J. Virol.*, **81**,
694 8374–8383.

695 31. Ichihara,M., Murakumo,Y., Masuda,A., Matsuura,T., Asai,N., Jijiwa,M., Ishida,M.,
696 Shinmi,J., Yatsuya,H., Qiao,S., *et al.* (2007) Thermodynamic instability of siRNA duplex

29

697   is a prerequisite for dependable prediction of siRNA activities. *Nucleic Acids Res.*, **35**,
698   e123–e123.

699 32. Wilson,J.A. and Richardson,C.D. (2005) Hepatitis C Virus Replicons Escape RNA
700   Interference Induced by a Short Interfering RNA Directed against the NS5b Coding
701   Region. *J. Virol.*, **79**, 7050–7058.

702 33. Hopcraft,S.E., Azarm,K.D., Israelow,B., Lévêque,N., Schwarz,M.C., Hsu,T.-H.,
703   Chambers,M.T., Sourisseau,M., Semler,B.L. and Evans,M.J. (2015) Viral Determinants
704   of miR-122-Independent Hepatitis C Virus Replication. *mSphere*, **1**.

705 34. Luna,J.M., Scheel,T.K.H., Danino,T., Shaw,K.S., Mele,A., Fak,J.J., Nishiuchi,E.,
706   Takacs,C.N., Catanese,M.T., de Jong,Y.P., *et al.* (2015) Hepatitis C Virus RNA
707   Functionally Sequesters miR-122. *Cell*, **160**, 1099–1110.

708 35. Doudna,J.A. and Charpentier,E. (2014) The new frontier of genome engineering with
709   CRISPR-Cas9. *Science*, **346**.

710 36. Wilson,J.A., Zhang,C., Huys,A. and Richardson,C.D. (2011) Human Ago2 Is Required
711   for Efficient MicroRNA 122 Regulation of Hepatitis C Virus RNA Accumulation and
712   Translation. *J. Virol.*, **85**, 2342–2350.

713 37. Reuter,J.S. and Mathews,D.H. (2010) RNAstructure: software for RNA secondary
714   structure prediction and analysis. *BMC Bioinformatics*, **11**, 129.

715 38. Darty,K., Denise,A. and Ponty,Y. (2009) VARNA: Interactive drawing and editing of the
716   RNA secondary structure. *Bioinformatics*, **25**, 1974–1975.

717 39. Thibault,P.A., Huys,A., Amador-Cañizares,Y., Gailius,J.E., Pinel,D.E. and Wilson,J.A.
718   (2015) Regulation of Hepatitis C Virus Genome Replication by Xrn1 and MicroRNA-
719   122 Binding to Individual Sites in the 5′ Untranslated Region. *J. Virol.*, **89**, 6294–6311.

720 40. Bernier,A. and Sagan,S.M. (2019) Beyond sites 1 and 2, miR-122 target sites in the HCV
721   genome have negligible contributions to HCV RNA accumulation in cell culture. *J. Gen.*
722   *Virol.*, **100**, 217–226.

723 41. Nasheri,N., Singaravelu,R., Goodmurphy,M., Lyn,R.K. and Pezacki,J.P. (2011)
724   Competing roles of microRNA-122 recognition elements in hepatitis C virus RNA.
725   *Virology*, **410**, 336–344.

726 42. Jopling,C.L. (2008) Regulation of hepatitis C virus by microRNA-122. *Biochem. Soc.*
727   *Trans.*, **36**, 1220–1223.

728 43. Schult,P. (2017) Functional Dissection of the Hepatitis C Virus Non-Structural Proteins
729   and miR-122 in Viral Replication and Translation.

730   44. Sarnow,P. and Sagan,S.M. (2016) Unraveling the Mysterious Interactions Between
731   Hepatitis C Virus RNA and Liver-Specific MicroRNA-122. *Annu. Rev. Virol.*, **3**, 309–
732   332.

733   45. Mortimer,S.A. and Doudna,J.A. (2013) Unconventional miR-122 binding stabilizes the
734   HCV genome by forming a trimolecular RNA structure. *Nucleic Acids Res.*, **41**, 4230–
735   4240.

736

737

738

739

740

741

742   **FIGURE LEGENDS:**

743

744   **Figure 1: HCV 5' UTR RNA structures (A).** Schematic representation of HCV 5'UTR stem

745   loops; SLI, SLIIa, SLIIb, SLIII and SLIV are indicated. Predicted structure of the 5' 117 nucleotide

746   RNA fragment alone forms a non-canonical RNA structure **(B).** and after annealing of 2 copies of

747   miR-122 forms the canonical structure **(C).** The miR-122 binding nucleotides are shown within

748   black boxes. Stem loops indicated in Red are parts of IRES.

749

750   **Figure 2: HCV replication promotion by siRNAs binding to nucleotides 10-47 in 5'UTR. (A)**

751   Diagrammatic representation of HCV genome showing 5'UTR polyprotein coding region and 3'

752   UTR. The first 55 nucleotides of HCV 5' UTR are shown interacting with 2 copies of miR-122

753   (green). siRNAs designed to walk the 5'UTR with single nucleotide resolution are represented.

754   Black lines represent siRNAs that do not promote replication and red lines represent ones that do.

755   **(B)** Diagram depicting the siRNA suppression assay. **(C)** siRNA suppression assay results with

756   siControl (grey bar), bars are colour coded based on their suppression activities. siRNAs that do

757   not suppress translation (black bars) and that suppress translation (red bars). **(D and E)** The pro-

758   viral activity of the siRNAs was assessed using HCV replication assays in which the activity of

759   miR-122 is antagonized using anti-miR-122. Ago2 knockout cells were co-electroporated with

760   HCV J6/ JFH-1(p7-Rluc2a) RNA, anti-miR-122 and the indicated siRNA and harvested at 2 hours

761   (grey bars), 24 hours (light grey bars), 48 hours (blue bars) and 72 hours (red bars) post-

762   electroporation. HCV replication was measured based on Rluc expression and is presented as %

763   relative to Rluc expression from HCV RNA supported by endogenous miR-122 at 72 hours post

764   electroporation (Endo miR-122). The data are the average of at least 3 independent experiments

765   and error bars represent the standard deviation. Statistical significance was determine using one-

766   way ANOVA on the relative 72-hour values where, *P<0.0332; **P< 0.0021; ***P < 0.0002;

767   ****P < 0.0001. **(F).** Heat map showing small-RNA efficiencies to promote virus replication. Red

768   signal means highest efficiency and yellow signals mean lowest efficiencies. Secondary structure

769   of HCV 1-47 nucleotides is shown to visualize the effect of small-RNA location binding on HCV

770   replication efficacy.

771

772   **Figure 3: The pro-and antiviral activity of siRNAs binding to the HCV IRES**. **(A)** A diagram

773   of the HCV IRES including stem loops II, III and IV and the locations of annealing of six siRNAs

774   that target the IRES are shown in red. **(B)** The pro-viral activity of the siRNAs was assessed using

775   replication assays in which the activity of miR-122 is antagonized by anti-miR-122. Ago2

776   knockout cells were electroporated with HCV J6/JFH-1(p7-Rluc2a) RNA, anti-miR-122 and the

777   indicated siRNA and harvested at 2 hours (grey bars), 24 hours (light grey bars), 48 hours (blue

778   bars) and 72 hours (red bars) post-electroporation. **(C)** The pro- or anti-viral effects of the indicated

779   siRNAs was assessed based on their influence on miR-122-independent replication of a U25C

780   mutant J6/JFH-1(p7-Rluc2a) similar to the experiments described in B. For B and C, HCV

781   replication was measured based on Rluc expression and is presented as % relative to Rluc

782   expression from HCV RNA supported by endogenous miR-122 at 72 hours post electroporation

783   (Endo miR-122). The data are the average of at least 3 independent experiments and error bars

784   represent the standard deviation. Statistical significance was determine using one-way ANOVA

785   on the relative 72 hour values where, *P<0.0332; **P< 0.0021; ***P < 0.0002; ****P < 0.0001.

786

Figure 4: The influence on HCV replication of siRNAs that binding at other predicted miR-122 binding. (A, B) Diagrammatic representation of HCV NS5B coding region and 3'UTR region secondary structures. The figure shows siRNAs (red) binding to other predicted miR-122 binding sites in NS5B coding region (left) and 3'UTR region (right). **(C)** The activity of the siRNAs was assessed using replication assays in which the activity of miR-122 is antagonized by anti-miR-122. Ago2 knockout cells were electroporated with HCV J6/JFH-1(p7-Rluc2a) RNA, anti-miR-122 and the indicated siRNA and harvested at 2 hours (grey bars), 24 hours (light grey bars), 48 hours (blue bars) and 72 hours (red bars) post-electroporation. HCV replication was measured based on Rluc expression and is presented as % relative to Rluc expression from HCV RNA supported by endogenous miR-122 at 72 hours post electroporation (Endo miR-122). Data represent the average of 3 independent experiments and error bars represent the standard deviation. Statistical significance was determine using one-way ANOVA on 72-hour values where, *$P<0.0332$; **$P< 0.0021$; ***$P < 0.0002$; ****$P < 0.0001$.

Figure 5: 5' UTR RNA structure predictions following annealing of the siRNAs that promote and do not promote HCV replication. Structure predictions of the HCV 5' terminal 117 nucleotides with annealing of the indicated siRNA was performed using online software RNAstructure, specific algorithm bifold. The first six lowest delta free energy structures obtained from predictions with each siRNAs are shown. The delta free energy calculated by the software is shown below each structure.

Figure 6: The minimum annealing requirements of siRNAs with si19-37 analogues (A) Diagrammatic representation of first 55 nucleotides of HCV 5' UTR are shown interacting with 2

810   copies of miR-122 (green). Sequences of si19-37 analogues at their binding positions are shown

811   and the number of annealing nucleotides for each analogue siRNA is indiacated. siRNAs in red

812   promote HCV replication and siRNAs in black do not promote HCV replication. Small lettered

813   characters in siRNAs show mismatched nucleotides that do not bind on HCV RNA (grey) while

814   capital lettered characters are nucleotides that bind on the RNA. The green box shown around

815   nucleotides 23-35 which were common in case of all siRNAs that promote HCV replication. **(B**

816   **and C)** The activity of the si19-37 analogues was assessed using replication assays in which the

817   activity of miR-122 is antagonized by anti-miR-122. Ago2 knockout cells were electroporated

818   with HCV J6/JFH-1(p7-Rluc2a) RNA, anti-miR-122 and the indicated siRNA and harvested at 2

819   hours (grey bars), 24 hours (light grey bars), 48 hours (blue bars) and 72 hours (red bars) post-

820   electroporation. HCV replication was measured based on Rluc expression and is presented as %

821   relative to Rluc expression from HCV RNA supported by endogenous miR-122 at 72 hours post

822   electroporation (Endo miR-122). Data represent the average of 3 independent experiments and

823   error bars represent the standard deviation. Statistical significance was determined using one-way

824   ANOVA on 72-hour values where, *P<0.0332; **P< 0.0021; ***P < 0.0002; ****P < 0.0001.

825   **(D)** Structure predictions of the HCV 5' terminal 117 nucleotides with annealing of the si19-37

826   RNA analogues that promoted replication. Predictions are based on bifold in the online software

827   RNAstructure, the six lowest delta free energy structures obtained from predictions with each

828   siRNAs are shown. The delta free energy calculated by the software is shown below each structure.

829

830   **Figure 7: HCV replication promotion with siRNAs binding on HCV 5' terminus and an**

831   **siRNA generated 3' overhang. (A and D)** Diagram of the first 55 nucleotides of HCV 5' UTR

832   interacting with 2 copies of miR-122 (green). miR-122 binding sites on HCV genome are shown

833   in bold characters. Uppercase letters represent nucleotides in the siRNAs that anneal to the HCV

834   RNA and lowercase letters represent nucleotides that do not. **(A).** Sequences of si19-37, si1-3--21-

835   36 and si1-3mm--21-36 are shown. **(D).** Schematic representation of si no ovh1--21-36 and si miR

836   ovh1-3mm-21-36 binding on HCV genome. **(B and E).** Graphs showing HCV replication

837   promotion by siRNAs that bind or do not bind to the 5' terminus and with siRNAs that do or do

838   not generate a 3' overhang. Ago2 knockout cells were electroporated with HCV J6/JFH-1(p7-

839   Rluc2a) RNA, anti-miR-122 and the indicated siRNA and harvested at 2 hours (grey bars), 24

840   hours (light grey bars), 48 hours (blue bars) and 72 hours (red bars) post-electroporation. HCV

841   replication was measured based on Rluc expression and is presented as % relative to Rluc

842   expression from HCV RNA supported by endogenous miR-122 at 72 hours post electroporation

843   (Endo miR-122). Data represents the average 3 independent experiments and error bars represent

844   the standard deviation. Statistical significance was determine using one-way ANOVA on 72-hour

845   values where, $*P<0.0332$; $**P< 0.0021$; $***P < 0.0002$; $****P < 0.0001$. **(C and F)** RNA

846   structure predictions of the HCV 5' terminal 117 nucleotides with annealing of siRNAs that bind

847   or do not bind to 5' terminus and with siRNAs that do or do not generate a 3' overhang. Predictions

848   are based on bifold in the online software RNAstructure and the delta free energy calculated by

849   the software are shown below each structure.

850

851   **Figure 8: small RNAs annealing promotes translation of HCV. (A)** Phenotypic analysis of

852   DROSHA/Ago2 double KO cells. Graph showing HCV replication induction by siRNAs in

853   DROSHA KO cells vs DROSHA/Ago2 double KO cells. **(B)** Western blot images showing the

854   absence Ago2 protein in DROSHA/Ago2 double KO cells vs the presence of Ago2 protein in

855   DROSHA KO cells. Uncropped blot is shown in Supplement Figure 2C **(C)** Transient translation

856   assays performed in DROSHA/Ago2 double KO cells using non-replicative viral RNA, J6/ JFH-

857   1(p7-Rluc2a) GNN, and the indicated siRNAs and an mRNA expressing Fluc as an electroporation

858   control. Samples were harvested at 4 hours and translation was accessed based on Rluc expression

859   vs the co-electroporated Fluc mRNA control. Data represent the average of at least 5 independent

860   experiments and error bars represent the standard deviation. Statistically significant differences

861   between siRNAs and siControl was assessed by one-way ANOVA, *P<0.0332; **P< 0.0021;

862   ***P < 0.0002; ****P < 0.0001. **(D)** Graph showing replication promotion at 72 hours post

863   infection by siRNAs used in the translation assays performed in Ago2 KO cells. **(C and D)** siRNAs

864   that promoted HCV translation and replication efficiently are coloured red, moderately efficient

865   ones are coloured orange and low efficient are coloured yellow. siRNAs that do not promote

866   replication are coloured black.

867

868   **Figure 9: Genome stabilization by small RNAs that do and do not promote HCV replication.**

869   **(A and B)** Northern blot analyses of HCV genomic RNA quantities during stability assays. Assays

870   are shown for HCV RNA with annealing of miR-122, two different siRNAs, or siControl. Bands

871   were quantified using ImageStudio Lite and were plotted as a one phase decay curve. These data

872   are representative of 2 independent experiments performed with each of the 4 siRNAs along with

873   control small RNAs (miR122 and sicontrol). Decay curves for each sample (miR-

874   122/siControl/19-37/si27-45/si15-33/si26-44) were generated independently and half-lives

875   obtained from these decay curves are mentioned. Full uncropped blots are shown in Supplement

876   Figure 2A. Decay curves and half-lives were calculated by Graphpad Prism.

877

878   **Figure 10: Summary model figure:**

879   We have developed a model for the mechanism of miR-122 promotion of HCV. In our model, the

880   (A). HCV 5' UTR RNA forms a non-canonical structure (colours of nucleotides represent small

881   RNA replication efficiency when bound to those nucleotides) in the absence of small RNA

882   annealing but (B). the canonical 5' UTR and IRES structure when bound with 2 copies of miR-

883   122 or with siRNAs. (A and B). Boxed nucleotides represent miR122 binding sites. Small RNA

884   induction or stabilization of the canonical IRES structure promotes virus translation leading to

885   enhanced virus replication. Small RNA annealing also stabilizes the viral genome, but genome

886   stabilization alone is not sufficient to promote the HCV lifecycle. We propose that small RNAs

887   anneal associate with host Argonaute proteins and together they are responsible for RNA structure

888   changes and viral genome stabilization. It is unknown if genome amplification is affected by miR-

889   122 or whether replication initiation is regulated by the canonical or non-canonical structures

890   (dotted arrow lines). All together we propose that a key role of miR-122 is to induce the canonical

891   5'UTR IRES structure and promote virus translation and that genome stabilization has a secondary

892   enhancing role but is insufficient alone.

893

894
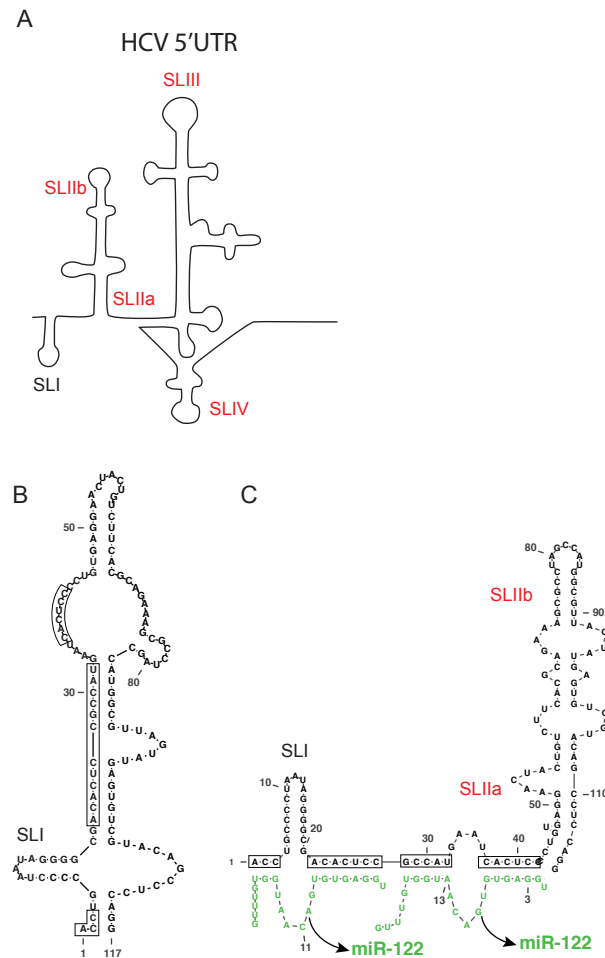
Figure 1: HCV 5' UTR RNA structures (A). Schematic representation of HCV 5'UTR stem loops; SLI, SLIIa, SLIIb, SLIII and SLIV are indicated. Predicted structure of the 5' 117 nucleotide RNA fragment alone forms a non-canonical RNA structure (B). and after annealing of 2 copies of miR-122 forms the canonical structure (C). The miR-122 binding nucleotides are shown within black boxes. Stem loops indicated in Red are parts of IRES.
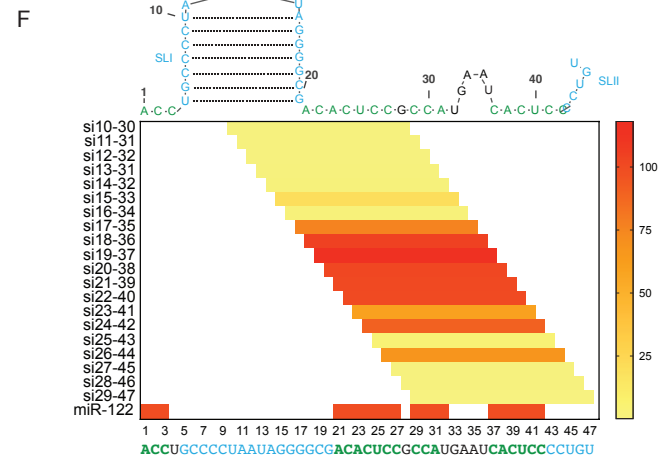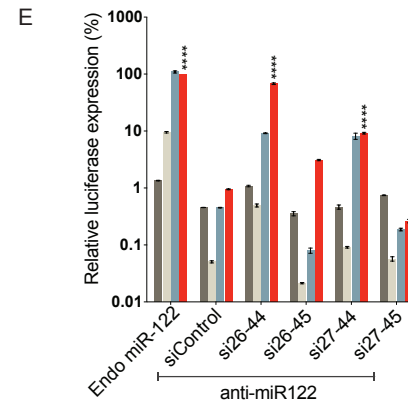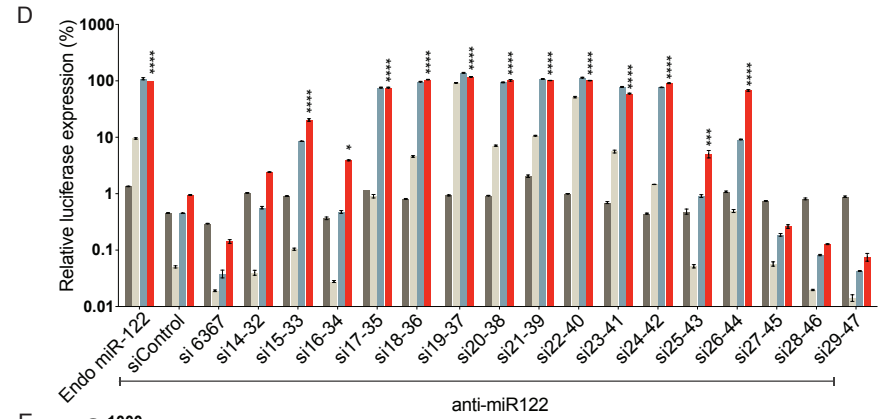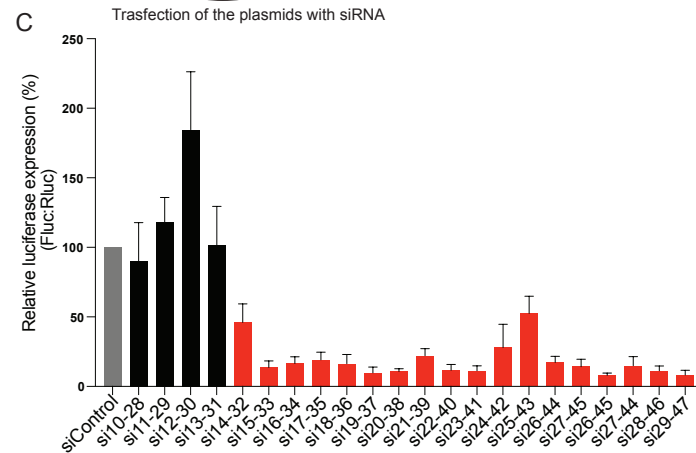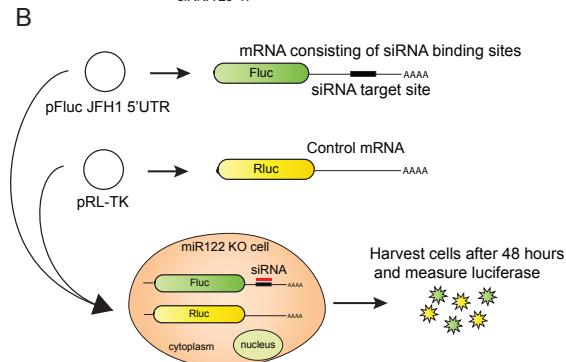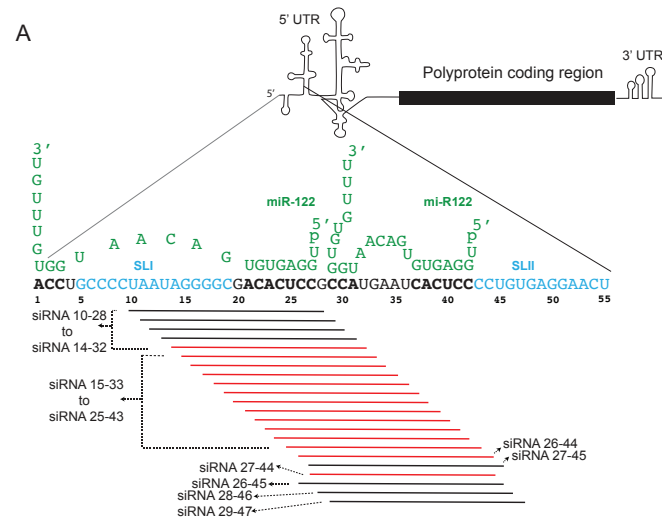
Figure 2: HCV replication promotion by siRNAs binding to nucleotides 10-47 in the 5'UTR. (A) Diagrammatic representation of HCV genome showing 5'UTR polyprotein coding region and 3' UTR. The first 55 nucleotides of HCV 5' UTR are shown interacting with 2 copies of miR-122 (green). siRNAs designed to walk the 5'UTR with single nucleotide resolution are represented. Black lines represent siRNAs that do not promote replication and red lines represent ones that do. (B) Diagram depicting the siRNA suppression assay. (C) siRNA suppression assay results with siControl (grey bar), bars are colour coded based on their suppression activities. siRNAs that do not suppress translation (black bars) and that suppress translation (red bars). (D and E) The pro-viral activity of the siRNAs was assessed using HCV replication assays in which the activity of miR-122 is antagonized using anti-miR-122. Ago2 knockout cells were co-electroporated with HCV J6/ JFH-1(p7-Rluc2a) RNA, anti-miR-122 and the indicated siRNA and harvested at 2 hours (grey bars), 24 hours (light grey bars), 48 hours (blue bars) and 72 hours (red bars) post-electroporation. HCV replication was measured based on Rluc expression and is presented as % relative to Rluc expression from HCV RNA supported by endogenous miR-122 at 72 hours post electroporation (Endo miR-122). The data are the average of at least 3 independent experiments and error bars represent the standard deviation. Statistical significance was determine using one-way ANOVA on the relative 72-hour values where, *$P<0.0332$; **$P< 0.0021$; ***$P < 0.0002$; ****$P < 0.0001$. (F). Heat map showing small-RNA efficiencies to promote virus replication. Red signal means highest efficiency and yellow signals mean lowest efficiencies. Secondary structure of HCV 1-47 nucleotides is shown to visualize the effect of small-RNA location binding on HCV replication efficacy.
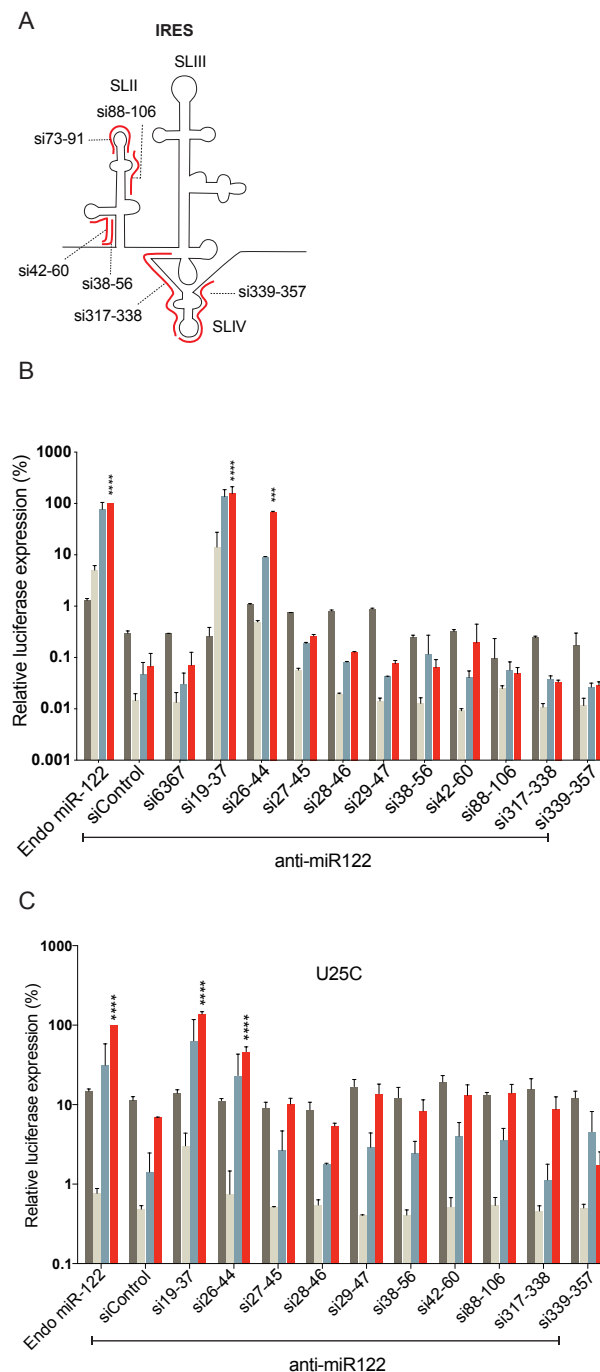
Figure 3: The pro-and antiviral activity of siRNAs binding to the HCV IRES. (A) A diagram of the HCV IRES including stem loops II, III and IV and the locations of annealing of six siRNAs that target the IRES are shown in red. (B) The pro-viral activity of the siRNAs was assessed using replication assays in which the activity of miR-122 is antagonized by anti-miR-122. Ago2 knockout cells were electroporated with HCV J6/JFH-1(p7-Rluc2a) RNA, anti-miR-122 and the indicated siRNA and harvested at 2 hours (grey bars), 24 hours (light grey bars), 48 hours (blue bars) and 72 hours (red bars) post-electroporation. (C) The pro- or anti-viral effects of the indicated siRNAs was assessed based on their influence on miR-122-independent replication of a U25C mutant J6/JFH-1(p7-Rluc2a) similar to the experiments described in B. For B and C, HCV replication was measured based on Rluc expression and is presented as % relative to Rluc expression from HCV RNA supported by endogenous miR-122 at 72 hours post electroporation (Endo miR-122). The data are the average of at least 3 independent experiments and error bars represent the standard deviation. Statistical significance was determine using one-way ANOVA on the relative 72 hour values where, *P<0.0332; **P< 0.0021; ***P < 0.0002; ****P < 0.0001.
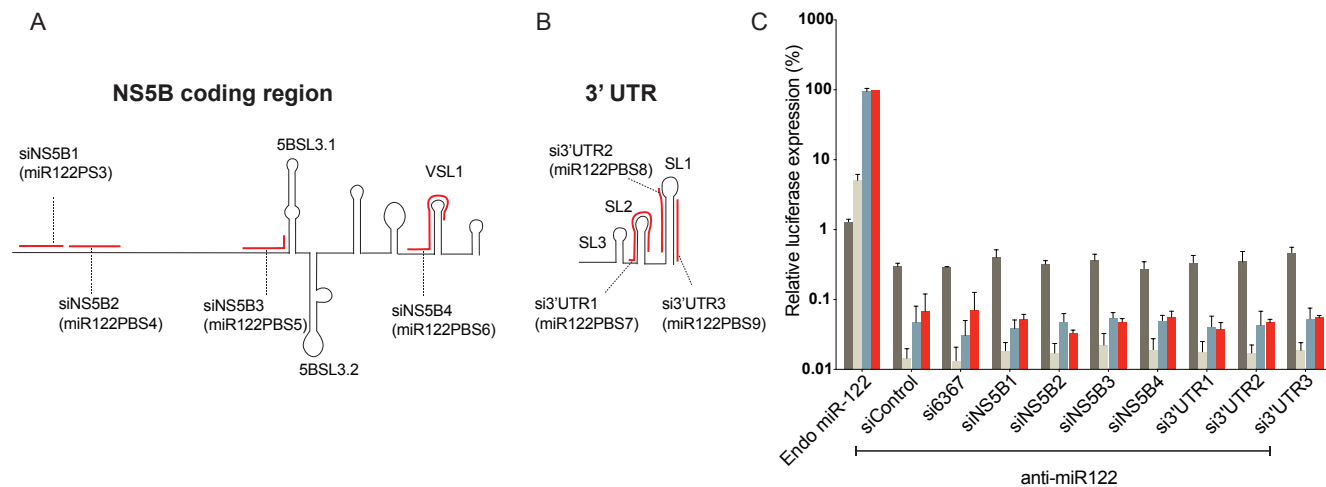
Figure 4: The influence on HCV replication of siRNAs that binding at other predicted miR-122 binding. (A, B) Diagrammatic representation of HCV NS5B coding region and 3'UTR region secondary structures. The figure shows siRNAs (red) binding to other predicted miR-122 binding sites in NS5B coding region (left) and 3'UTR region (right). (C) The activity of the siRNAs was assessed using replication assays in which the activity of miR-122 is antagonized by anti-miR-122. Ago2 knockout cells were electroporated with HCV J6/JFH-1(p7-Rluc2a) RNA, anti-miR-122 and the indicated siRNA and harvested at 2 hours (grey bars), 24 hours (light grey bars), 48 hours (blue bars) and 72 hours (red bars) post-electroporation. HCV replication was measured based on Rluc expression and is presented as % relative to Rluc expression from HCV RNA supported by endogenous miR-122 at 72 hours post electroporation (Endo miR-122). Data represent the average of 3 independent experiments and error bars represent the standard deviation. Statistical significance was determine using one-way ANOVA on 72-hour values where, *P<0.0332; **P< 0.0021; ***P < 0.0002; ****P < 0.0001.

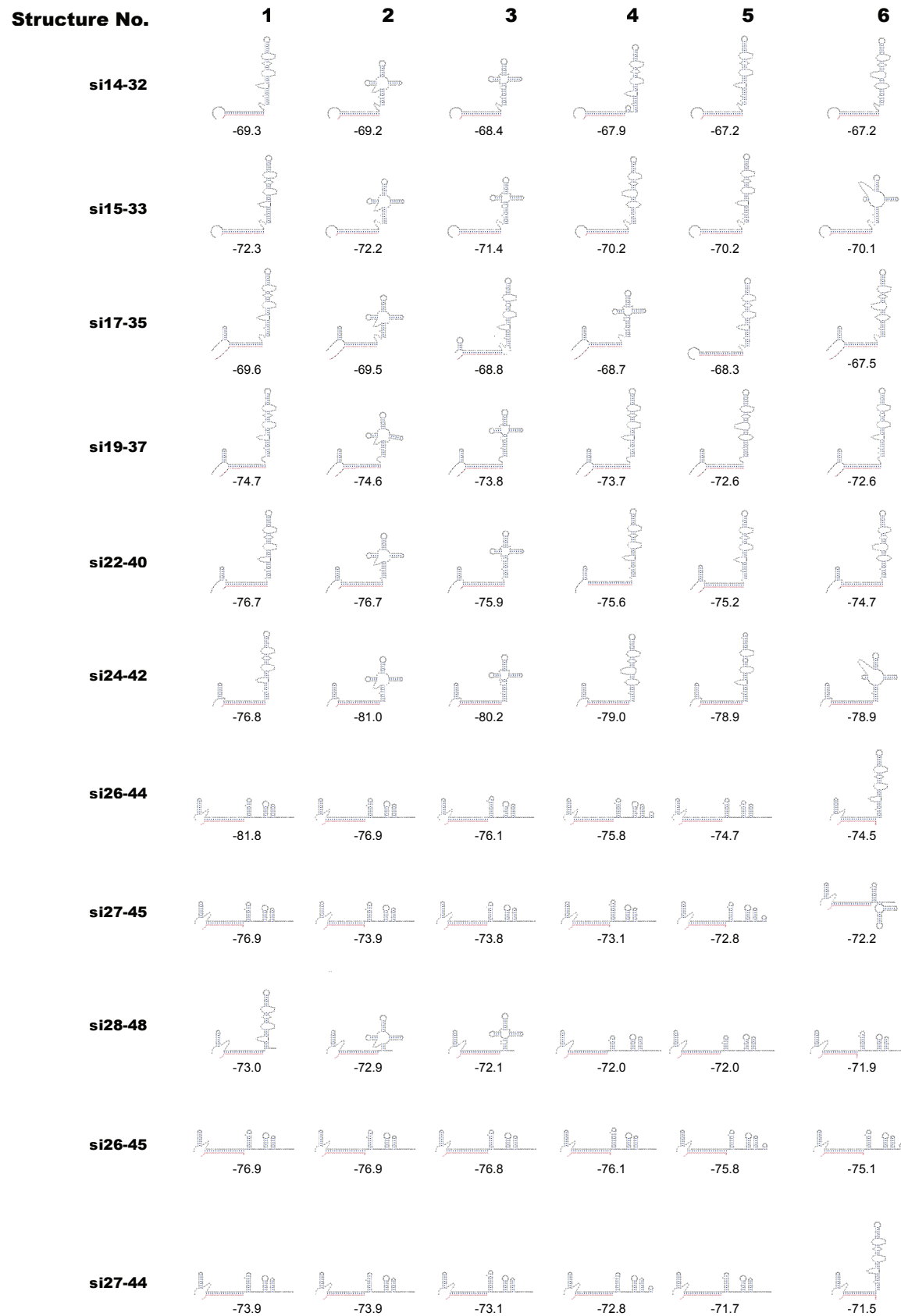| Structure No.	1	2	3	4	5	6
si14-32	-69.3	-69.2	-68.4	-67.9	-67.2	-67.2
si15-33	-72.3	-72.2	-71.4	-70.2	-70.2	-70.1
si17-35	-69.6	-69.5	-68.8	-68.7	-68.3	-67.5
si19-37	-74.7	-74.6	-73.8	-73.7	-72.6	-72.6
si22-40	-76.7	-76.7	-75.9	-75.6	-75.2	-74.7
si24-42	-76.8	-81.0	-80.2	-79.0	-78.9	-78.9
si26-44	-81.8	-76.9	-76.1	-75.8	-74.7	-74.5
si27-45	-76.9	-73.9	-73.8	-73.1	-72.8	-72.2
si28-48	-73.0	-72.9	-72.1	-72.0	-72.0	-71.9
si26-45	-76.9	-76.9	-76.8	-76.1	-75.8	-75.1
si27-44	-73.9	-73.9	-73.1	-72.8	-71.7	-71.5

Figure 5: 5' UTR RNA structure predictions following annealing of the siRNAs that promote and do not promote HCV replication. Structure predictions of the HCV 5' terminal 117 nucleotides with annealing of the indicated siRNA was performed using online software RNAstructure, specific algorithm bifold. The first six lowest delta free energy structures obtained from predictions with each siRNAs are shown. The delta free energy calculated by the software is shown below each structure.
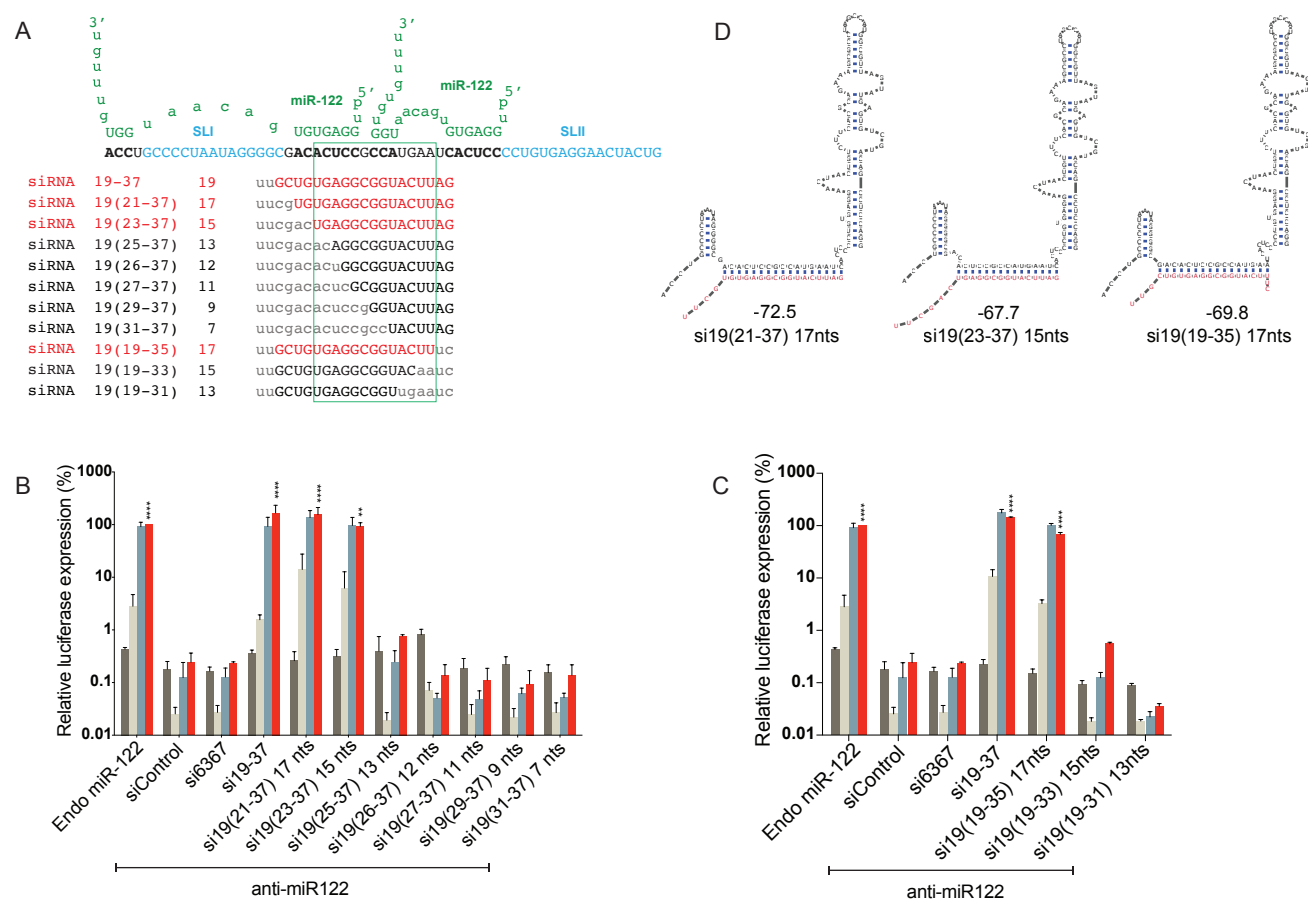
Figure 6: The minimum annealing requirements of siRNAs with si19-37 analogues. (A) Diagrammatic representation of first 55 nucleotides of HCV 5' UTR are shown interacting with 2 copies of miR-122 (green). Sequences of si19-37 analogues at their binding positions are shown and the number of annealing nucleotides for each analogue siRNA is indiacated. siRNAs in red promote HCV replication and siRNAs in black do not promote HCV replication. Small lettered characters in siRNAs show mismatched nucleotides that do not bind on HCV RNA (grey) while capital lettered characters are nucleotides that bind on the RNA. The green box shown around nucleotides 23-35 which were common in case of all siRNAs that promote HCV replication. (B and C) The activity of the si19-37 analogues was assessed using replication assays in which the activity of miR-122 is antagonized by anti-miR-122. Ago2 knockout cells were electroporated with HCV J6/JFH-1(p7-Rluc2a) RNA, anti-miR-122 and the indicated siRNA and harvested at 2 hours (grey bars), 24 hours (light grey bars), 48 hours (blue bars) and 72 hours (red bars) post-electroporation. HCV replication was measured based on Rluc expression and is presented as % relative to Rluc expression from HCV RNA supported by endogenous miR-122 at 72 hours post electroporation (Endo miR-122). Data represent

Figure 7: HCV replication promotion with siRNAs binding on HCV 5' terminus and an siRNA generated 3' overhang. (A and D) Diagram of the first 55 nucleotides of HCV 5' UTR interacting with 2 copies of miR-122 (green). miR-122 binding sites on HCV genome are shown in bold characters. Uppercase letters represent nucleotides in the siRNAs that anneal to the HCV RNA and lowercase letters represent nucleotides that do not. (A). Sequences of si19-37, si1-3--21-36 and si1-3mm--21-36 are shown. (D). Schematic representation of si no ovh1--21-36 and si miR ovh1-3mm-21-36 binding on HCV genome. (B and E). Graphs showing HCV replication promotion by siRNAs that bind or do not bind to the 5' terminus and with siRNAs that do or do not generate a 3' overhang. Ago2 knockout cells were electroporated with HCV J6/JFH-1(p7-Rluc2a) RNA, anti-miR-122 and the indicated siRNA and harvested at 2 hours (grey bars), 24 hours (light grey bars), 48 hours (blue bars) and 72 hours (red bars) post-electroporation. HCV replication was measured based on Rluc expression and is presented as % relative to Rluc expression from HCV RNA supported by endogenous miR-122 at 72 hours post electroporation (Endo miR-122). Data represents the average 3 independent experiments and error bars represent the standard deviation. Statistical significance was determine using one-way ANOVA on 72-hour values where, *$P<0.0332$; **$P< 0.0021$; ***$P < 0.0002$; ****$P < 0.0001$. (C and F) RNA structure predictions of the HCV 5' terminal 117 nucleotides with annealing of siRNAs that bind or do not bind to 5' terminus and with siRNAs that do or do not generate a 3' overhang. Predictions are based on bifold in the online software RNAstructure and the delta free energy calculated by the software are shown below each structure.
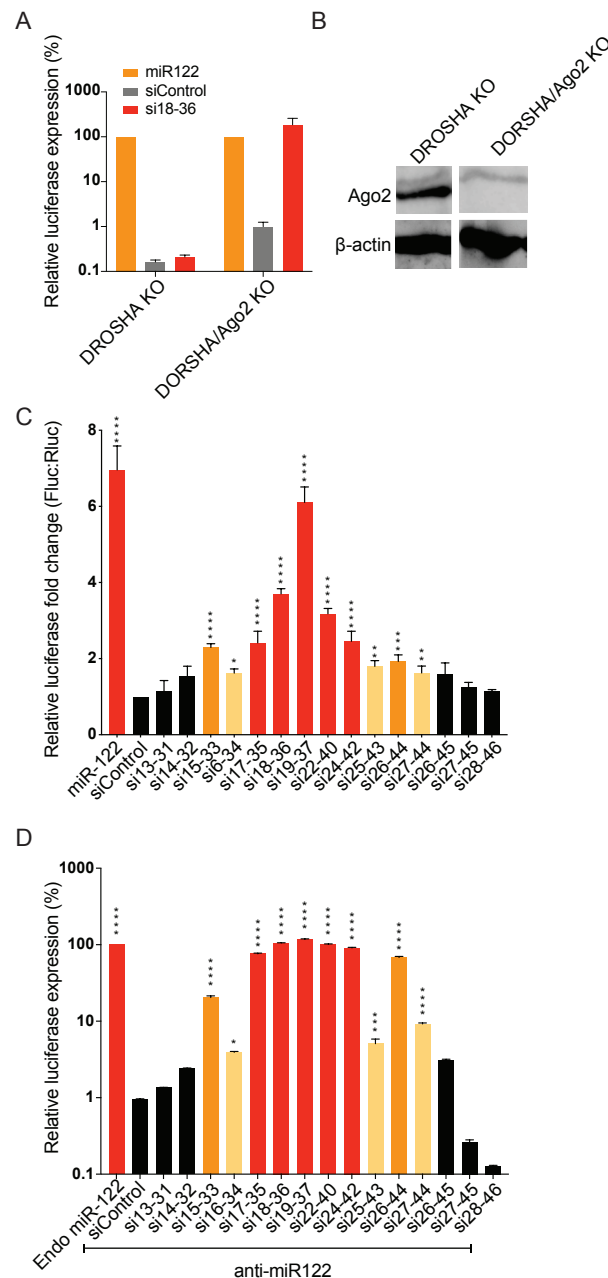
Figure 8: small RNAs annealing promotes translation of HCV. (A) Phenotypic analysis of DROSHA/Ago2 double KO cells. Graph showing HCV replication induction by siRNAs in DROSHA KO cells vs DROSHA/Ago2 double KO cells. (B) Western blot images showing the absence Ago2 protein in DROSHA/Ago2 double KO cells vs the presence of Ago2 protein in DROSHA KO cells. Uncropped blot is shown in Supplement Figure 2C (C) Transient translation assays performed in DROSHA/Ago2 double KO cells using non-replicative viral RNA, J6/ JFH-1(p7-Rluc2a) GNN, and the indicated siRNAs and an mRNA expressing Fluc as an electroporation control. Samples were harvested at 4 hours and translation was accessed based on Rluc expression vs the co-electropo-rated Fluc mRNA control. Data represent the average of at least 5 independent experiments and error bars represent the standard deviation. Statistically significant differences between siRNAs and siControl was assessed by one-way ANOVA, *P<0.0332; **P< 0.0021; ***P < 0.0002; ****P < 0.0001. (D) Graph showing replication promotion at 72 hours post infection by siRNAs used in the translation assays performed in Ago2 KO cells. (C and D) siRNAs that promoted HCV translation and replication efficiently are coloured red, moderately efficient ones are coloured orange and low efficient are coloured yellow. siRNAs that do not promote replication are coloured black.
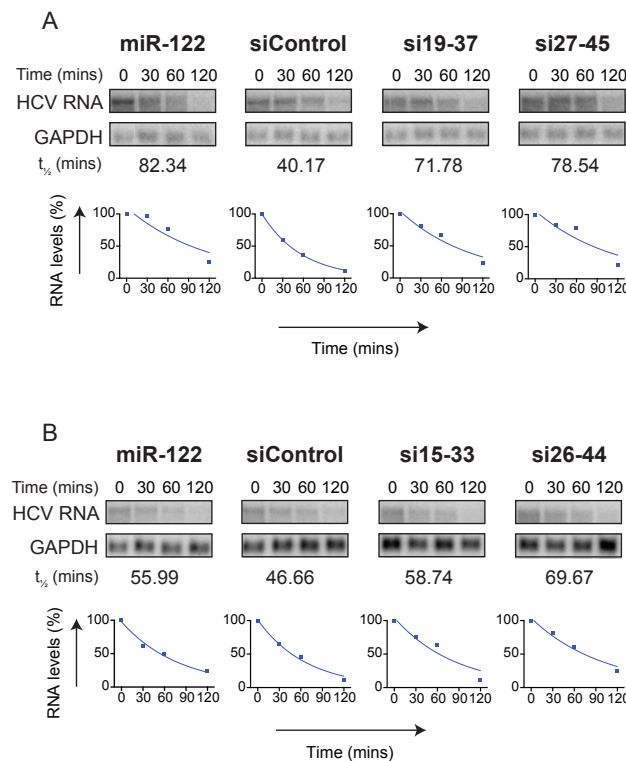
Figure 9: Genome stabilization by small RNAs that do and do not promote HCV replication. (A and B) Northern blot analyses of HCV genomic RNA quantities during stability assays. Assays are shown for HCV RNA with annealing of miR-122, two different siRNAs, or siControl. Bands were quantified using Image-Studio Lite and were plotted as a one phase decay curve. These data are representative of 2 independent experiments performed with each of the 4 siRNAs along with control small RNAs (miR122 and sicontrol). Decay curves for each sample (miR-122/siControl/19-37/si27-45/si15-33/si26-44) were generated independently and half-lives obtained from these decay curves are mentioned. Full uncropped blots are shown in Supplement Figure 2A. Decay curves and half-lives were calculated by Graphpad Prism.
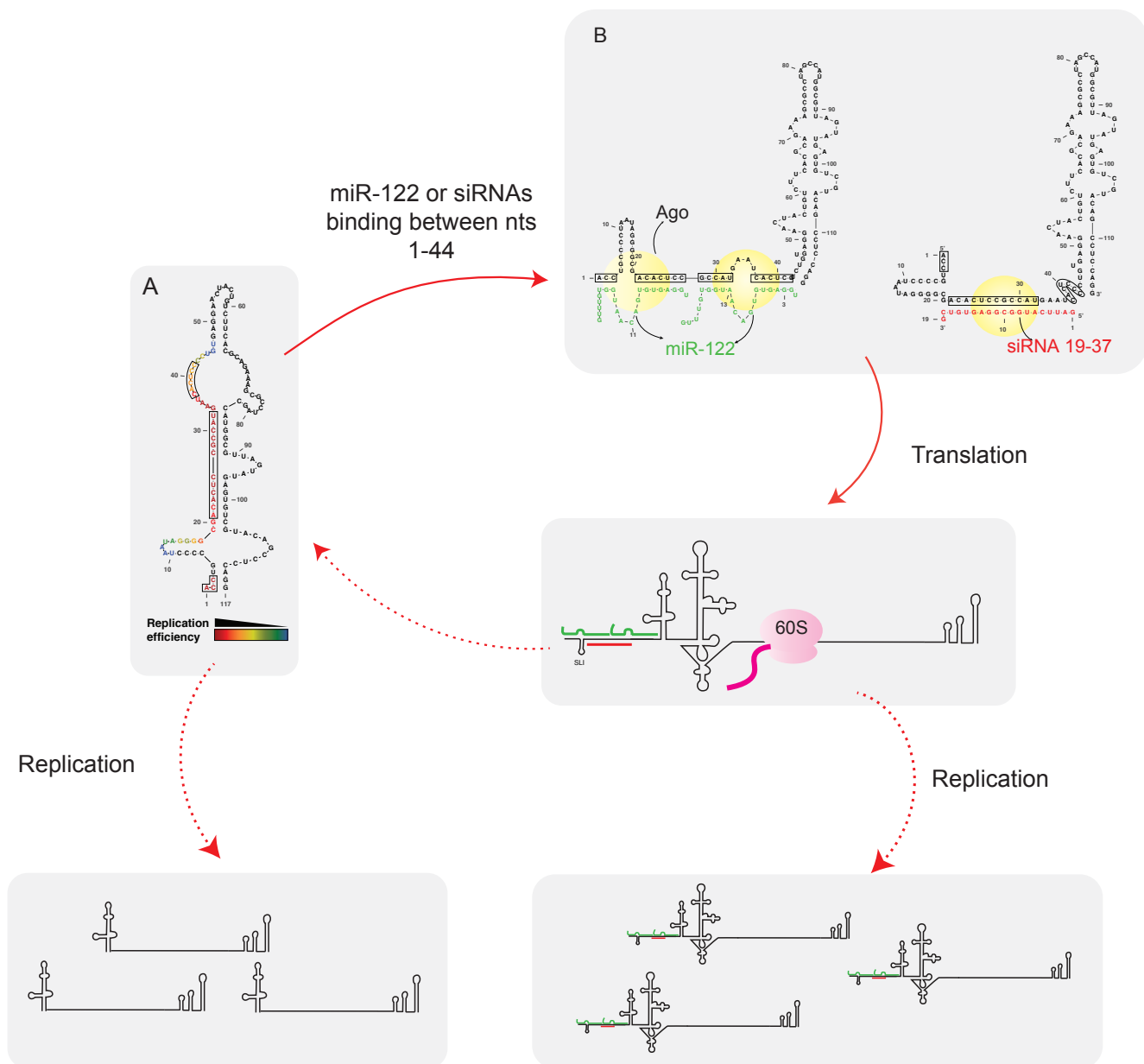
Figure 10: Summary model figure: We have developed a model for the mechanism of miR-122 promotion of HCV. In our model, the (A). HCV 5' UTR RNA forms a non-canonical structure (colours of nucleotides represent small RNA replication efficiency when bound to those nucleotides) in the absence of small RNA annealing but (B). the canonical 5' UTR and IRES structure when bound with 2 copies of miR-122 or with siRNAs. (A and B). Boxed nucleotides represent miR122 binding sites. Small RNA induction or stabilization of the canonical IRES structure promotes virus translation leading to enhanced virus replication. Small RNA annealing also stabilizes the viral genome, but genome stabilization alone is not sufficient to promote the HCV lifecycle. We propose that small RNAs anneal associate with host Argonaute proteins and together they are responsible for RNA structure changes and viral genome stabilization. It is unknown if genome amplification is affected by miR-122 or whether replication initiation is regulated by the canonical or non-canonical
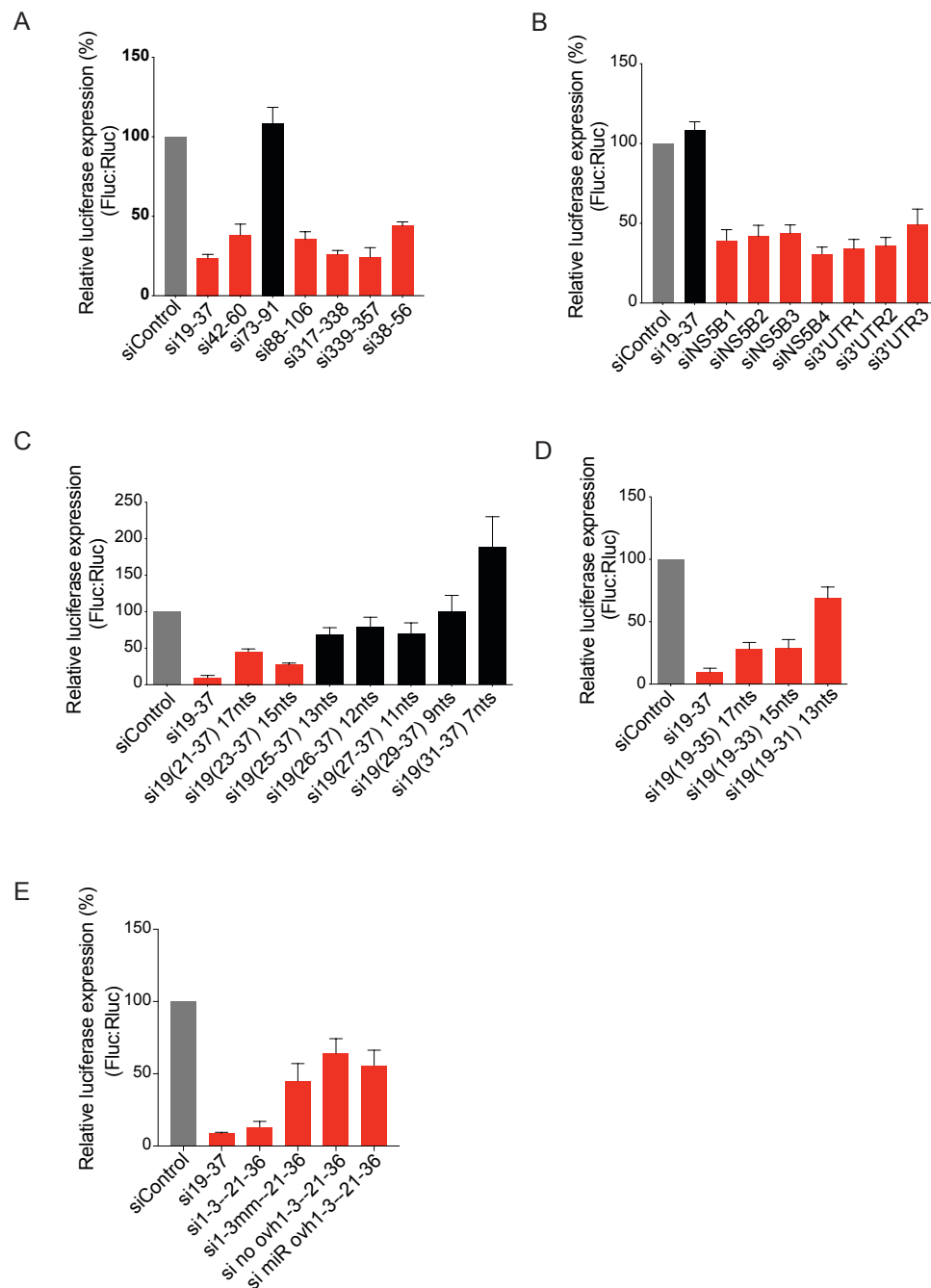
Supplement Figure 1: SiRNA suppression assays for A.) siRNAs that bind within the HCV IRES B.) siRNAs that bind within NS5B and the 3'UTR C and D.) si19-37 analogues E.) siRNAs tested for terminal binding and overhang. Red bars indicate siRNAs that suppress translation, black bars indicate siRNAs that do not suppress translation.
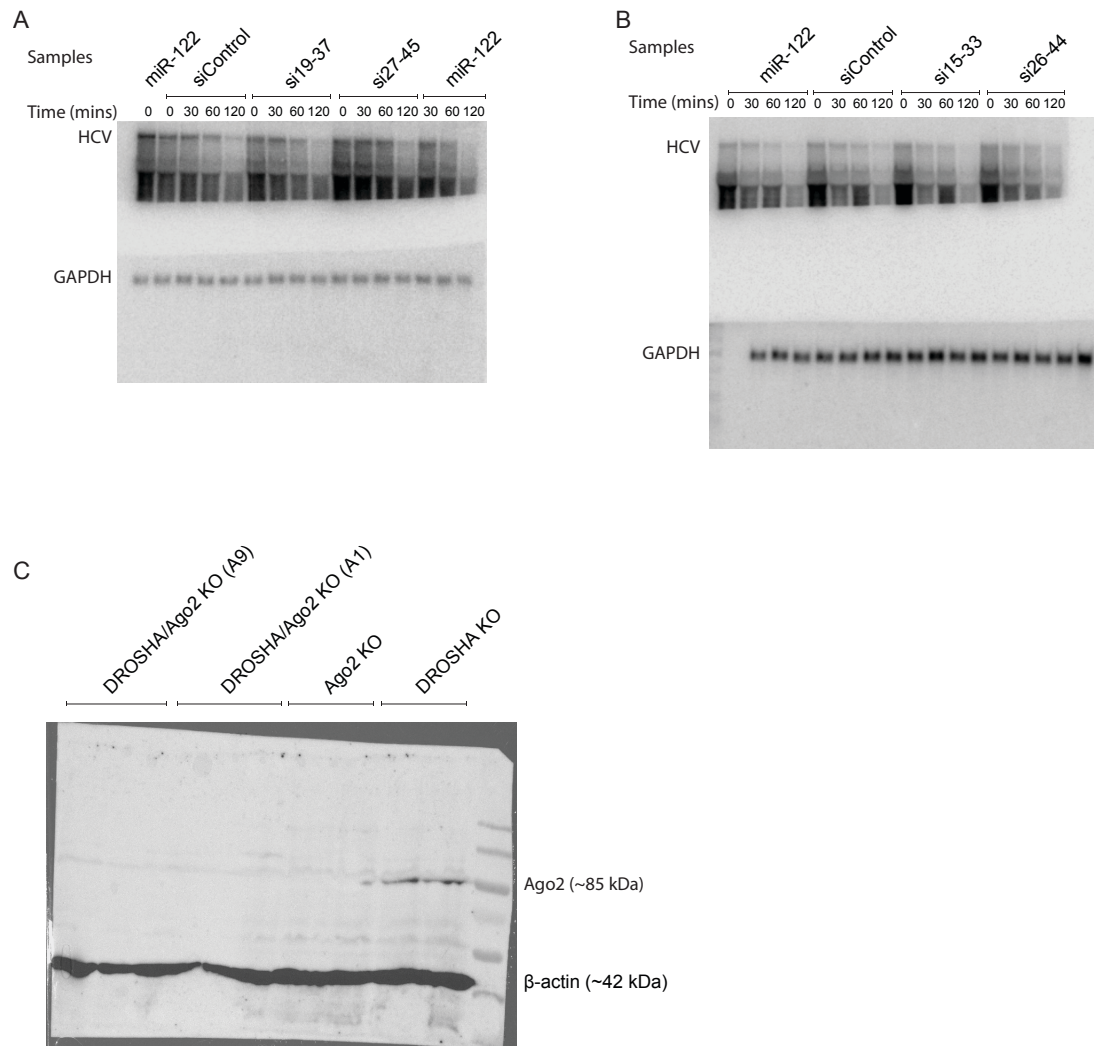
Supplement Figure 2: A.) and B.) Northern blot membranes for experiments describes in Stabilization assay. C.) Western blot described to assess expression of Ago2 protein in DROSHA/Ago2 KO cells. DROSHA/Ago2 cell clone A9 was used for our studies.

Supplementary Table 1:

	Suppression/siRNA activity	Canonical structure formation	Replication	Translation	Stabilization
miR-122	Y	Y	H	H	Y
si10-28	N	N	N	ND	ND
si11-29	N	N	N	ND	ND
si12-30	N	N	N	ND	ND
si13-31	N	N	N	ND	ND
si14-32	Y	N	N	N	ND
si15-33	Y	N	I	I	Y
si16-34	Y	N	L	L	ND
si17-35	Y	Y	H	H	ND
si18-36	Y	Y	H	H	ND
si19-37	Y	Y	H	H	Y
si20-38	Y	Y	H	ND	ND
si21-39	Y	Y	H	ND	ND
si22-40	Y	Y	H	H	ND
si23-41	Y	Y	H	ND	ND
si24-42	Y	Y	H	H	ND
si25-43	Y	Y	L	L	ND
si26-44	Y	Y	I	I	Y
si27-44	Y	Y	L	L	ND
si26-45	Y	N	N	N	ND
si27-45	Y	N	N	N	Y
si28-46	Y	N	N	N	ND
si29-47	Y	N	N	ND	ND

Y = Yes, N = No, H = High, I = intermediate and L = Low, ND = not done

Supplementary Table 2:

siRNAs	Formation of SLI	Formation of SLIIa	Formation of SLIIb	Formation of UK-SL	Replication efficiency
miR122	YES	YES	YES	NO	High
si11-29	NO	YES	YES	YES	No
si13-31	NO	YES	YES	YES	No
si14-32	NO	YES	YES	YES	No
si15-33	NO	YES	YES	NO	Intermediate
si17-35	YES	YES	YES	NO	High
si19-37	YES	YES	YES	NO	High
si20-38	YES	YES	YES	NO	High
si22-40	YES	YES	YES	NO	High
si24-42	YES	YES	YES	NO	High
si26-44	YES	YES	YES	NO	Intermediate
si27-44	YES	YES	YES	NO	Low
si26-45	YES	NO	NO	NO	No
si27-45	YES	NO	NO	NO	No
si28-46	YES	NO	YES	NO	No

Canonical structure formation = presence of SLI, SLIIa and SLIIb; absence of UK-SL (unknown stem loop)

Supplementary Table 3: small RNAs used in this study

RNAs	Sequence (5' – 3')
miR–122	UGGAGUGUGACAAUGGUGUUUGU
5' UTR siRNAs	
si10–30	CGGAGUGUCGCCCCUAUUAUU
si11–29	GGCGGAGUGUCGCCCCUAUUU
si12–30	GCGGAGUGUCGCCCCUAUUUU
si13–31	UGGCGGAGUGUCGCCCCUAUU
si14–32	AUGGCGGAGUGUCGCCCCUUU
si15–33	CAUGGCGGAGUGUCGCCCCUU
si16–34	UCAUGGCGGAGUGUCGCCCUU
si17–35	UUCAUGGCGGAGUGUCGCCUU
si18–36	AUUCAUGGCGGAGUGUCGCUU
si19–37	GAUUCAUGGCGGAGUGUCGUU
si20–38	UGAUUCAUGGCGGAGUGUCUU
si21–39	GUGAUUCAUGGCGGAGUGUUU
si22–40	AGUGAUUCAUGGCGGAGUGUU
si23–41	GAGUGAUUCAUGGCGGAGUUU
si24–42	GGAGUGAUUCAUGGCGGAGUU
si25–43	GGGAGUGAUUCAUGGCGGAUU
si26–44	GGGGAGUGAUUCAUGGCGGUU
si27–45	AGGGGAGUGAUUCAUGGCGUU
si26–45	AGGGGAGUGAUUCAUGGCGGUU
si27–44	GGGGAGUGAUUCAUGGCGUU
si28–46	CAGGGGAGUGAUUCAUGGCUU
si29–47	ACAGGGGAGUGAUUCAUGGUU
IRES binding siRNAs	
si38–56	UAGUUCCUCACAGGGGAGUUU
si42–60	ACAGUAGUUCCUCACAGGGUU
si73–91	AACGCCAUGGCUAGGCGCUUU
si88–106	UACGACACUCAUACUAACGUU
si317–338	UGCACGGUCUACGAGACCUCCCUU
si339–357	UUAGGAUUUGUGCUCAUGGUU
NS5B-3'UTR binding siRNAs	

`siNS5B 1`	`GGCGAGUGGAGUGGUUGGGUU`
`siNS5B 2`	`GAUAGGGGAGUGUCUAACUUU`
`siNS5B 3`	`CCGGCAAUGGAGUGAGUUUUU`
`si3'UTR 1`	`UUAGCUAUGGAGUGUACCUUU`
`si3'UTR 2`	`UUUCACAGCUAGCCGUGACUU`
`si3'UTR 3`	`UACGGCACUCUCUGCAGUCUU`
`si3'UTR 4`	`AUGAUCUGCAGAGAGACCAUU`
Terminus binding and overhang siRNAs	
`si1-3—21-36: Terminus binding`	`AUUCAUGGCGGAGUGUGGUUU`
`si 1-3mm—21-36: Non-terminus binding`	`AUUCAUGGCGGAGUGUCCAUU`
`si miR ovh1-3--21-36: overhang siRNA`	`AUUCAUGGCGGAGUGUGGUGUUUGU`
`si no ovh1-3--21-36: overhang siRNA`	`AUUCAUGGCGGAGUGUGGU`
Minimum annealing requirement siRNAs	
`si19(21-37) _17`	`GAUUCAUGGCGGAGUGUGCUU`
`si19(23-37) _15`	`GAUUCAUGGCGGAGUCAGCUU`
`si19(25-37) _13`	`GAUUCAUGGCGGACACAGCUU`
`si19(26-37) _12`	`GAUUCAUGGCGGUCACAGCUU`
`si19(27-37) _11`	`GAUUCAUGGCGCUCACAGCUU`
`si19(29-37) _9`	`GAUUCAUGGGCCUCACAGCUU`
`si19(31-37) _7`	`GAUUCAUCCGCCUCACAGCUU`
`si19(19-35) _17`	`CUUUCAUGGCGGAGUGUCGUU`
`si19(19-33) _15`	`CUAACAUGGCGGAGUGUCGUU`
`si19(19-31) _13`	`CUAAGUUGGCGGAGUGUCGUU`